



Tracking Body Movements while Undergoing a Sit-to-stand Maneuver

Report no. 1

Under-Graduate Final Project

Submitted toward the degree of

Bachelor of Science in Biomedical Engineering

By

Peretz Shahar

Asraf Shani

Supervised by Prof. Geffen Amit & Maayan Lustig

July 2023

Table of Content

1 Abstract	4
2 Introduction	4
2.1 The Problem	5
2.2 The StS Action	5
2.2.1 Physiology	5
2.2.2 The Challenges and Differences in Performing StS	7
2.3 Motion Capture Systems	10
2.3.1 Motion Capture System based on LiDAR sensor.....	10
3 Objectives.....	11
4 Materials and Methods.....	12
4.1 Experimental and Computational Models Assumptions	12
4.2 Motion Capture System Design for Sit-to-Stand Analysis using LiDAR sensor 15	
4.2.1 Calibration of the LiDAR sensor.....	15
4.2.2 Design a new method for motion capture system.....	17
4.3 The Experimental Protocol	19
4.3.1 The Experimental Setup	19
4.3.2 StS maneuver without using the SnS device	20
4.3.3 StS maneuver with the support of the SnS device.....	22
4.4 Outcome Measures	23
4.4.1 Signal Processing.....	23
4.4.2 Statistical Analysis	24
4.4.3 Qualitative Analysis	25
5 Results	26
5.1 Calibration of the LiDAR sensors	26
5.2 1 st Experiment Session Results.....	28
5.2.1 Information regarding the Experimental Participants	28
5.2.2 The SnS device effect on the CoM position	29
5.2.3 Modeling StS maneuver	30
5.2.4 Evaluation of the SnS Device's Effect by the Models	35
5.3 2 nd Experiment Session Results (Post Protocol Improvements).....	37
5.3.1 Information regarding the Experimental Participants	37
5.3.2 The SnS device effect on the CoM position	38
6 Discussion	44
7 Conclusion.....	50
8 References	53
9 Appendix	56
9.1 Appendix A – Per Subject Analysis	56
9.1.1 Subject 1	56
9.1.2 Subject 2	58
9.1.3 Subject 3	59
9.1.4 Subject 4	61
9.1.5 Subject 5	63
9.1.6 Subject 6	65

9.1.7	Subject 7	67
9.1.8	Subject 8	69
9.2	comprehensive evaluation of the StS movement with the SnS device.....	72
9.3	MATLAB code for the LiDAR calibration	73
9.4	MATLAB code for the StS analysis.....	75
9.4.1	Extract StS sections from the signals	75
9.4.2	Calculate the computational assumptions and the statistical measurments.	78
9.4.3	Plot 2 dimensional graphs	82

1 Abstract

Sit-to-Stand (StS) is the most common daily functional activity. During the natural ageing process, changes occur in the sensorimotor systems which affects the performance of StS transition and often lead to falls. Therefore, there are external assisting devices that help in performing StS, such as SitnStand (SnS) device. Additionally, there are different biomechanical motion assessment methods to track mobility and stability while performing StS, but their clinical deployment is limited by the required hardware, time, and expertise .Accordingly, the goal of this project is to establish a new method of a motion capture system which would be portable, cheap, and easy to operate and one that requires simple data processing. The method is based on the light detection and ranging (LiDAR) sensor which exist in several smart phones. Using this method, the safety and reliability of SnS device tested. According to corresponding protocol and system-based LiDAR sensor, an experiment was conducted on 8 subjects (63-72 years old). The results were analyzed using MATLAB software for general movement characterization as well as for assessing SnS device effect. The tested method for capturing motion meet the requirements and resulted in a quality movement description of StS. Alongside this, it is not possible to decide on the relevance of all the computational assumptions as well as the effect of SnS device. The most promising computational assumption is the AUC measurement, especially when measured on signals provided from y-axis (when LiDAR's beam was directing to the ceiling). A follow-up experiment with a larger number of relevant subjects should be conducted.

2 Introduction

The introduction provides an overview of the challenges associated with performing and measuring the daily action of sit-to-stand (StS) in older adults. It begins by discussing the prevalence and consequences of the phenomenon among older adults, followed by a description of the physiology of the StS action and the difficulties older adults may experience while performing it. The introduction then goes on to explain how SS can be identified in laboratory tests, and introduces the SitnStand (SnS) device, which is designed to assist in performing the StS action. Finally, it covers the current methods for motion capture, their associated challenges, and proposes a new, portable, inexpensive, and easy-to-use motion capture system that requires minimal data processing.

2.1 The Problem

Sitting-to-standing (StS) is the most common daily functional activity and is a prerequisite for other many activities. StS is an important component of independent upright mobility and a key component of independent living [1],[2]. Healthy adults need to perform 60 ± 22 StS motions every day [1],[3-6].

Over 18% of Americans over 65 have limited mobility. Two million people have difficulty getting up from a chair without assistance [7]. It has been found that over half of older people living in Long-Term Care (LTC) have difficulty rising from a seated position to a standing position independently, with approximately 10% of falls occurring while attempting to rise from sitting [8]. Moreover, in elderly adults, poor StS performance has been identified as a predictor of fall risk [4],[9],[10]. According to a report published in 2018, each year, an estimated 29 million adults ages 65 and older fall. Meaning an older adult falls every second of every day [11]. Falls among adults 65 and older caused over 34,000 deaths in 2019, making it the leading cause of injury death for that group. In addition, in 2019, the emergency department recorded 3 million visits for older adult falls. Therefore, if rates continue to rise such as the last years, it can anticipate for 7 fall death every hour by 2030. Besides, older adult falls cost \$50 billion in medical costs annually [12].

2.2 The StS Action

2.2.1 Physiology

Standing up is a complex activity. The motion can be defined as the transfer of support from the seat to the feet, or as the transfer from a stable position to a less stable posture (moving from a stable 3-point base to a stable 2-point base) [7],[13],[14]. In StS movements, the center of mass (CoM) momentum must be controlled to maintain balance within the base of support (BoS) [1],[10]. Dynamic models have been developed to describe the transition of the subject to a stable standing position based on the dynamics and biomechanics of the StS action. These models estimate the subject's stability based on the locations of the CoM and the BoS [13],[15]. A common approach separated the standing action into four phases (Fig.1): **(I) Flexion-momentum** - The initial rotation of the hips and pelvis forward. Initiating the movement and lifting the posterior from the chair seat are the beginning and ending of this phase. The beginning of StS cycle corresponds to

fast changes in the anterior-posterior component of the ground reaction force. For normal and fast StS, the movement can be considered as closer to a ballistic movement, and forward momentum generation is necessary to transfer weight from the seat to the feet.

(II)Momentum-transfer - Consist of the forward momentum of the CoM being converted into vertical momentum. The movement begins with the posterior being lifted and ends with maximal ankle dorsiflexion. The starting of the seat-unloading phase is detected by rapid positive changing in vertical ground reaction forces. The seat unloading phase is part of the vertical acceleration of the body mass. At the instant of seat-off the anterior-posterior ground reaction force reaches its maximal value. **(III)Vertical extension** - The vertical rise of the CoM to a standing position. As soon as the ankle is fully extended, this phase starts and ends with the hips stopping to extend, including leg and trunk extension. **(IV)Stabilization** - Consist of settling of any postural sway in the CoM. During this phase, hip extension is reached and then all motions connected to stabilization are achieved. The standing on moment is detected when the vertical ground reaction force fluctuation does not exceed $\pm 1\%$ of the bodyweight [2],[16-18].

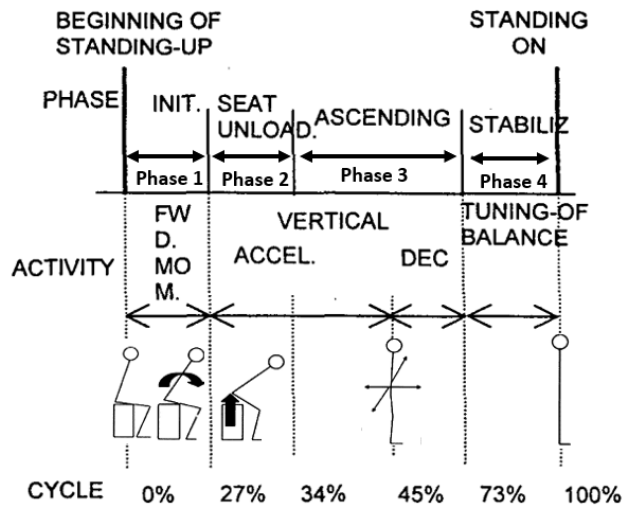


Figure 1 - StS cycle diagram, phase, activity, and event marker definitions. Forward momentum (FWD. MOM), acceleration (ACCEL), deceleration (DEC)[18]

Many parameters can be measured during StS, such as velocity, angular velocity, momentum, ground reaction force, angle changes and distance changes (e.g., horizontal - Δx , vertical- Δy) [19]. Below (Fig. 2) is a typical example of ground reaction force change over time [20].

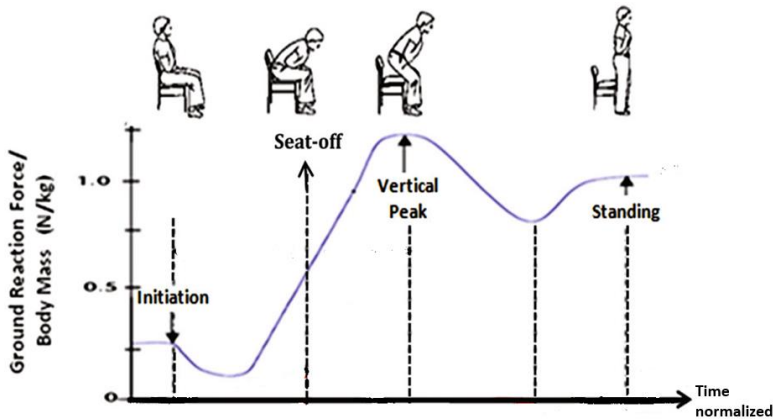


Figure 2 - a typical example of a StS vertical and anteroposterior force–time curve recorded from a force platform [20].

2.2.2 The Challenges and Differences in Performing StS

During the natural ageing process, changes occur in the sensorimotor systems that result in a gradual decrease in strength, joint mobility, and balance, as well as a decrease in multimodal sensory processing, which affects the performance of StS transition (whether it's with or without pathology) [2]. Physical impairments due diseases also make StS difficult [7],[13],[14],[21].

There is a relationship between changes in the motor control of StS task, which appeared during periods of potential postural instability, and the effects of ageing on postural stability [22]. Across age groups, trunk motion is similar. It may be interpreted as an invariant characteristic of the StS maneuver in aiming to produce the horizontal momentum of the CoM to achieve a standing posture, and as a way of minimizing the effects of destabilization generated by rapid displacements of trunk [22],[23]. Despite this similarity, trunk velocity profiles in elderly subjects are less smooth than in young subjects, with numerous accelerations, particularly after seat-off and during the acceleration phases orientated in the opposite direction to gravity (forward bending deceleration and backward returning acceleration). In addition, there was a change in knee angular velocity at the start of the deceleration phase of trunk forward displacement after seat-off (Fig. 3).

Individuals experiencing difficulties in a StS task have been observed to prioritize postural stability by adopting a slower upward motion [24]. It was found that older individuals who struggled with StS movements initiated their seat-off with a reduced velocity compared to their physically capable counterparts. This slower initiation aimed

to mitigate the destabilizing effect caused by forward momentum when the CoM approached the boundary of the BoS in the forward direction. In general, an inability to effectively generate and control the velocity and acceleration of the CoM during StS leads to poor management of body momentum, resulting in imbalance [25]. Hence, it was suggested that analyzing CoM velocity and acceleration can provide valuable insights into the control of balance during StS tasks [10],[25].

Significantly, a smaller forward CoM velocity and acceleration as the CoM nears the point directly above the BoS, as well as minimal crossover of the CoM above the BoS (to avoid or minimize progression ahead of the forefoot) during the rising phase, indicate better neuromuscular control over the body's stability [26]. In simpler terms, a safe StS requires the CoM to ascend slowly and gradually above the BoS, maintain minimal fluctuations above the BoS once in position, and avoid moving ahead of the BoS.

In elderly subjects' modifications of kinematic parameters can be interpreted as alterations of postural control. Moreover, elderly subjects required more time than young subjects to achieve the task (Elderly subjects spent a greater time performing each phase than young subjects). Generally considered a feature of ageing, motor slowing has been studied during psychomotor tasks and in complex activities [22].

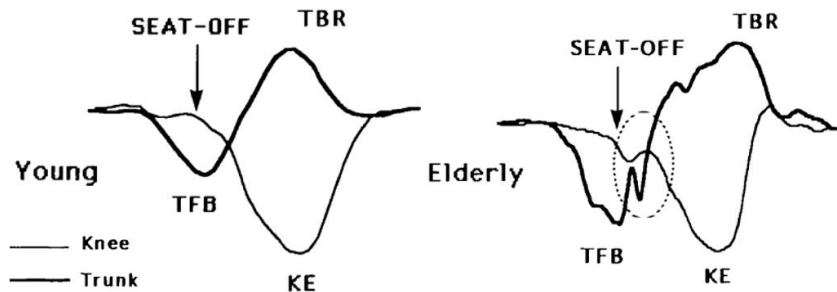


Figure 3 - Typical angular velocity profiles of the trunk (—) and the knee (—) for one younger (top) and one older subject (bottom). The arrows indicate seat-off and seat-on events and the dotted circles indicate main modifications of velocity profiles in elderly

Old people could suffer falls due to the failure to perform StS movements. As well as ageing, during StS movement, differences about Ground Reaction Forces (GRF) between single fallers (a subject testified that he fell once during last year) and non-fallers (a subject testified that he didn't fall during last year) have been seen (Fig. 4) [27].

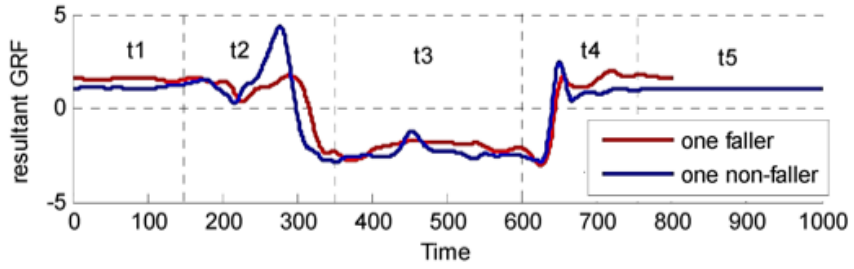


Figure 4 - GRF on the force plate during StS movement. At the beginning of StS movement, the person keeps on stand (t_1). The time from stand to sit on t_2 , from sit to stand on t_4 . The curves for faller are smoother than the non-faller, with lower peak [27].

The difficulty in getting up from a chair is attributed to phase II because many parameters must be controlled within a short time frame (9% of StS cycle). At seat-off (the transition between phase I. and II.), people are typically statically unstable. A healthy subject usually swings their torso forward for forward momentum, which helps move the CoM over the BoS dynamically and facilitates standing through the statically unstable region. In contrast, this phase for elderly subjects can be difficult, unless they are adopting a different strategy or using external assistance [15]. In addition, the stabilization phase (phase IV) seems to represent the moment of specific relevance during StS necessary for the distinction between elderly and young subjects [28]. In the rising phases (phases II & III) falls were twice as common as in the stabilization phase (Phase IV). The most common reason for falls during sit-to-stand transfers is imbalance during the rising phases. However, injuries were more likely to occur during the subsequent stabilization phase. While falls during stabilization are more likely to be sideways, falls during rising are more likely to be backward [8].

Designing a device to facilitate this motion without requiring assistance by others is one means of helping the elderly and disabled to do StS motion [3], [13], [21], [29]. SnS is a portable aid for lifting a chair suitable for different types of seats. The aid is a pillow that inflates in 4 stages up to a height and angle, which bring the CoM to an easier starting point for the start of StS [30].

2.3 Motion Capture Systems

The clinical deployment of biomechanical motion assessment is limited by the required hardware, time, and expertise. It is typically performed in dedicated laboratory spaces, using motion-capture, such as: video analysis with/without markers [3], [6], [13-15], Electromyography (EMG) analysis, use of optoelectronic systems - e.g., VICON 612 optical motion analysis system with markers [21], goniometry, and accelerometry; and force-sensing systems. Moreover, it is required data-analysis and processing systems that are dedicated to musculoskeletal analysis [15]. In addition, the measuring mostly based on measuring biomechanical factors, such as angles and moments of individual joints or body weight distribution at points of contact [6].

The goal of the project is to establish a new method of a motion capture system which would be portable, cheap, and easy to operate and one that requires simple data processing. The method is based on the light detection and ranging (LiDAR) sensor which already exist in several smart phones today (such as the iPhone 13 Pro), so that StS tests could be performed anywhere, without the need of high expertise, and in a user-friendly way. Using this method of motion assessment, the safety and reliability of SnS device could be tested easily and reliably for quality assurance purposes of the device.

2.3.1 Motion Capture System based on LiDAR sensor

In addition to the motion capture systems discussed, it is also possible to use different sensors and techniques to track motion and evaluate it. For example, the LiDAR sensor can be used in order to measure the changes within movement by calculating the differences in distance during the motion. LiDAR is an optical remote sensing technique which determines the distance from an object or surface by pulsing optical lasers. The LiDAR sensor consists of a laser, a scanner, and a detector. The laser emits a beam of light, which is directed towards the target by the scanner. The scanner can be mounted on a rotating platform, allowing the LiDAR sensor to scan a wide area [31]. When the laser beam hits the target, it is reflected to the detector, which measures the time it took for the beam to return. The LiDAR system uses the time it takes for a laser pulse to travel to a target and back to measure the distance between the sensor and the target. When the laser pulse hits the target, it is reflected to the sensor. The speed of light is constant, so by

measuring the time it takes for the pulse to return, the LiDAR system can accurately determine the distance to the target. It is similar to radar, but uses electromagnetic radiation at a higher frequency, and works in the ultraviolet, visible, and infrared parts of the spectrum. This technique uses UV radiation, visible or close to infrared light to image verity kinds of objects. The advantage of this technique is the fact that it uses wavelength that are well reflected by small objects. One can control the wavelength and by that adjust the reflection for the desired application. The laser typically has a very narrow beam that allows physical features to be mapped at very high resolution compared to the radar. The LiDAR sensor can measure the distance to the target with high accuracy, making it a useful tool for mapping and navigation. It can also be used to measure the velocity of moving objects, as well as the shape and surface characteristics of the target [32].

The LiDAR sensor has been incorporated into iPhone cell phones starting from the "Pro" models. According to Apple's documentation on the current specifications of iPhone Pro models, the LiDAR scanning capability extends up to a range of 16 feet, equivalent to approximately 5 meters, with a field of view of 90 degrees. The sensor measurement accuracy is within 5 mm of the true distance from the sensor [33]. Additionally, from an evaluation of the sensor's accuracy performed by Apple et al., it appears that the sensor has an error in precision of 1cm, and the precision is decreasing as the scanning surface decrease under 10 cm side length and the limit of detection for objects is around 5 m [34].

3 Objectives

The main goal is to examine the new motion capture system based on LiDAR sensor that planed and design through this project. Accordingly, the monitoring of the movement would be examined both with and without explicit reference to the use of SnS device.

Moreover, specifically, to develop research evidence for the safety and effectiveness of the SnS device in reducing the user risks associated with rising up from a chair, the following two research hypotheses will be experimentally tested:

- (1) **Non-inferiority hypothesis:** The use of SnS does not increase the Risk of Falling (RoF) for the user during rise up compared to the rising up from the same chair without using the SnS as an aid.

(2) Superiority hypothesis: The use of SnS decreases the RoF for the user during rise up compared to the rising up from the same chair without using the SnS as an aid.

4 Materials and Methods

In order to demonstrate the effectiveness of the SnS device in reducing the RoF during the StS motion from a chair, an experimental setup was devised. This setup involved tracking the StS motion using a LiDAR sensor integrated into iPhones (Pro series), followed by a comprehensive analysis and evaluation of the StS motion using biomechanical metrics.

4.1 Experimental and Computational Models Assumptions

We have developed the following mathematical expressions to quantify the movement and determine whether the SnS device is effective in decreasing the RoF during the StS motion when rising up from a chair [36]:

(1) Area Under the Curve (AUC) of the CoM as function of time during StS maneuver.

$$\text{Eq. 1} \quad \min \int |\Delta[\text{CoM}]X(t)|dt$$

Where the $[\text{CoM}]X(t)$ is the distance of the Center of Mass from the surface in x axis

$$\text{Eq. 2} \quad \min \int |\Delta[\text{CoM}]Y(t)|dt$$

Where the $[\text{CoM}]Y(t)$ is the distance of the Center of Mass from surface in y axis

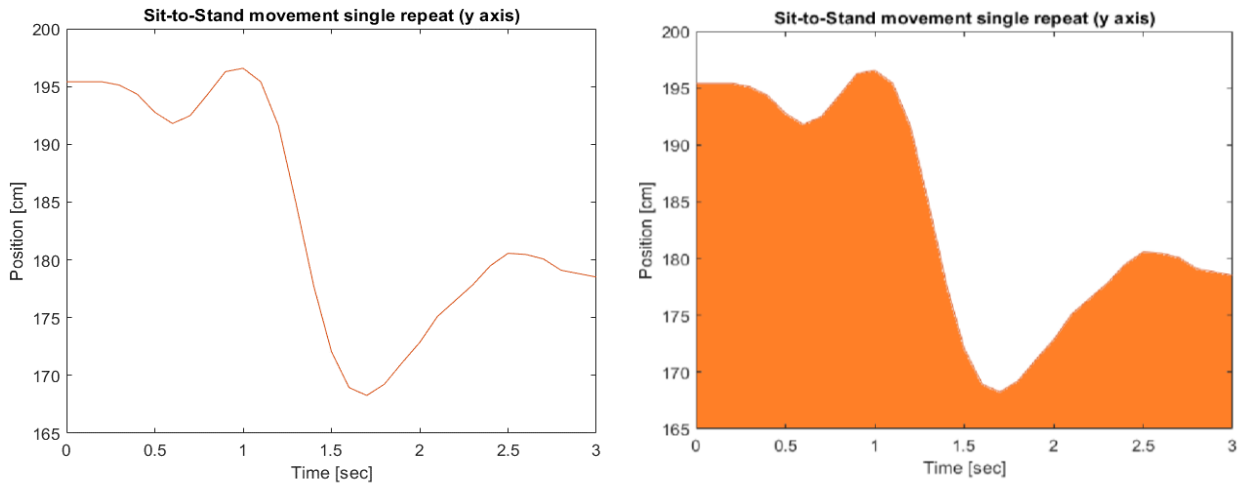


Figure 5 - visual description of the AUC definition. On the left; StS motion graph, on the right; AUC when applied on the motion graph

The position of the CoM is changing over time during the StS maneuver as the subject's CoM moves during the movement to gain stability of the entire action. The Equations calculate the integral of the distance between the CoM and a steady surface in two axes (x and y) over time while performing StS maneuver and it assumes that the smaller the integral the better the stability of the movement. The source of the assumption is that ideally, the $\Delta[CoM]x(t)$ and the $\Delta[CoM]y(t)$ are monotonically decreasing functions that has a maximal distance value when the person is seated (as the distances of the person's CoM from the surfaces in both axes are maximal when seated). A higher AUC may be due to fluctuations of the CoM that caused from difficulty to perform StS maneuver, as the CoM is the key factor for the body's stability and difficulty to gain stability during movement can result in CoM's fluctuations, as discussed in the introduction.

Of note, the amplitude and frequency of such fluctuations are indicators of the balance performance of the user during and post StS (with versus without the SnS device). A favorable outcome supporting hypothesis 1 would involve a reduction in both the horizontal and vertical sway of the CoM as it approaches the desired standing position. Consequently, a lower value of the AUC would suggest a smoother and safer motion.

(2) Velocity of the CoM as function of time during StS maneuver.

$$\text{Eq. 3} \quad \min\left\{\frac{d(\Delta[CoM]X(t))}{dt}\right\}$$

Where the $[CoM]X(t)$ is the distance of the Center of Mass from the surface in x axis and the derivative of this distance over time is being calculated

$$\text{Eq. 4} \quad \min\left\{\frac{d(\Delta[CoM]Y(t))}{dt}\right\}$$

Where the $[CoM]Y(t)$ is the distance of the Center of Mass from the surface in y axis and the derivative of this distance over time is being calculated

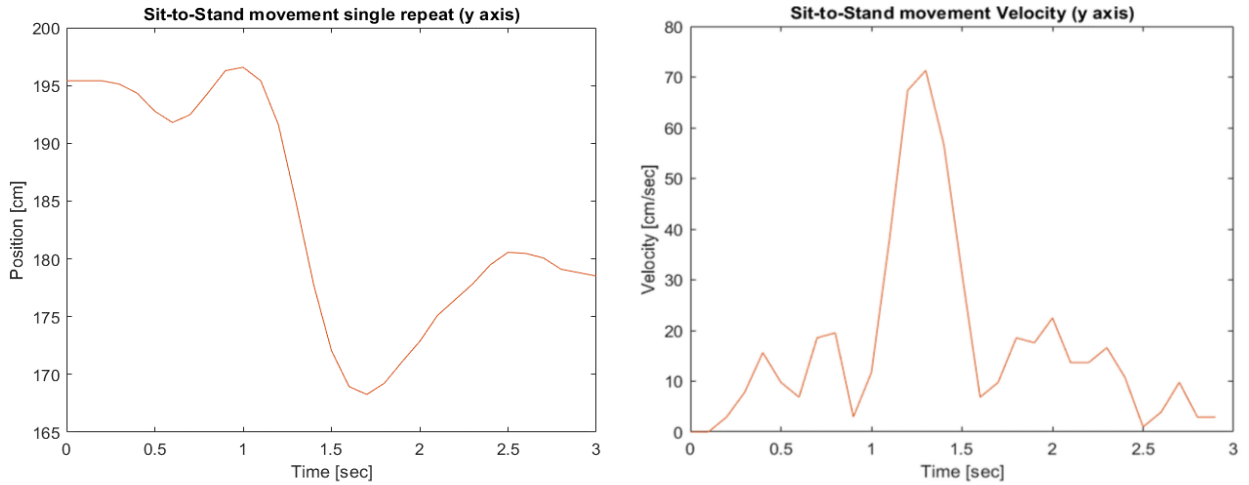


Figure 6 - visual description of the Velocity definition. On the left; StS motion graph, on the right; Velocity calculation when applied on the motion graph

The initial assumption was that the utilization of SnS device would aid the subject in performing the StS movement compared to performing the StS movement without the device's assistance. As described in the introduction, a poor ability to control the velocity and acceleration of the CoM during StS leads to poor management of body momentum, resulting in imbalance. Accordingly, a smaller forward CoM velocity and acceleration as the CoM reach above the BoS indicate better body's stability, which means that a safe StS requires the CoM to ascend slowly and gradually above the BoS [24],[25],[10],[26].

(3) Acceleration of the CoM as function of time during StS maneuver.

$$\text{Eq. 5} \quad \min\left\{\frac{d^2(\Delta[\text{CoM}]X(t))}{dt^2}\right\}$$

Where the $[\text{CoM}]X(t)$ is the distance of the Center of Mass from the surface in x axis and the second derivative of this distance over time is being calculated

$$\text{Eq. 6} \quad \min\left\{\frac{d^2(\Delta[\text{CoM}]Y(t))}{dt^2}\right\}$$

Where the $[\text{CoM}]Y(t)$ is the distance of the Center of Mass from the surface in y axis and the second derivative of this distance over time is being calculated

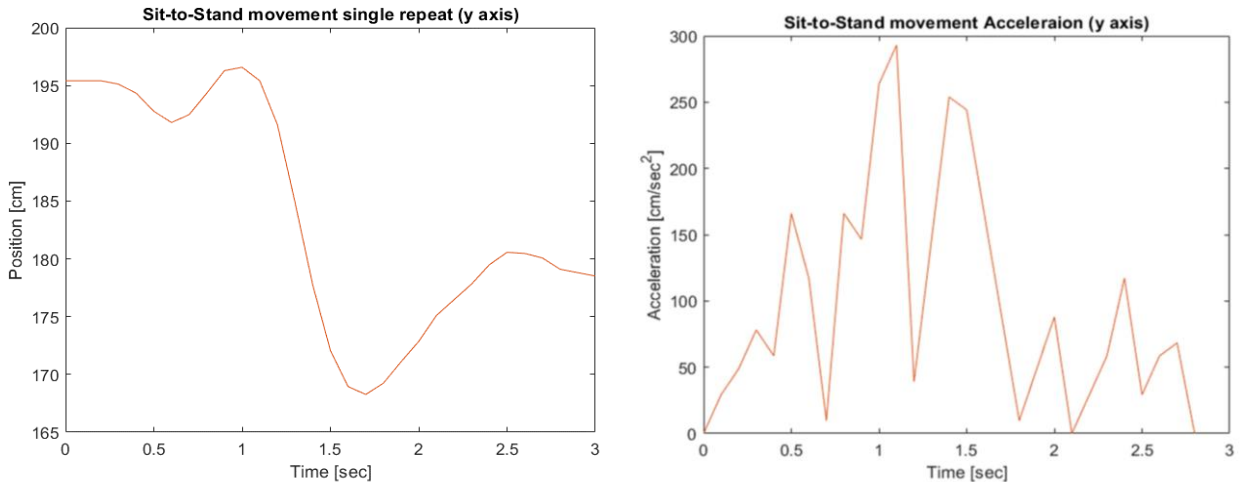


Figure 7 - visual description of the Acceleration definition. On the left; StS motion graph, on the right; Acceleration calculation when applied on this graph

It is expected that the velocity will be "smoother" when using the SnS device. Therefore, the acceleration, which expresses the degree of changes in velocity, expected to be lower (equations (5), (6)).

4.2 Motion Capture System Design for Sit-to-Stand Analysis using LiDAR sensor

The LiDAR sensor can be used as a tool to accurately measure distances between objects and assumed to effectively track person's movements. Accordingly, in order to use a LiDAR sensor as the key item in the motion capture system of this project, it was necessary to evaluate its performance and assess the reliability and credibility of the results obtained by the sensor. Additionally, in order to enable an accurate measurement with small as possible noises and errors during the measurement it was required to design system that enable tracking and recording of the StS maneuver accurately and easily without being based on complicated algorithms and massive data analysis.

4.2.1 Calibration of the LiDAR sensor

In order to evaluate the accuracy of the distance and velocity parameters measured by the iPhone Pro LiDAR sensor, a comparative analysis was conducted by comparing the sensor's measurements with a reference standard. Specifically, an iPhone Pro cell-phone was connected to a testing machine (Instron Corp., model 5544, Norwood, MA, USA) with a position control resolution of 0.008 m and speed range of 0.05-1000 mm/min [35]. The machine is connected to an operating software (BlueHill® software Instron

Corp.) which records the distance and velocity measurements, while simultaneously capturing the same measurements using the iPhone Pro LiDAR. The calibration process conducted as follows; first, the iPhone has been attached to the Instron machine using glutted tape and directed towards a white box, as demonstrated in Figure 8.

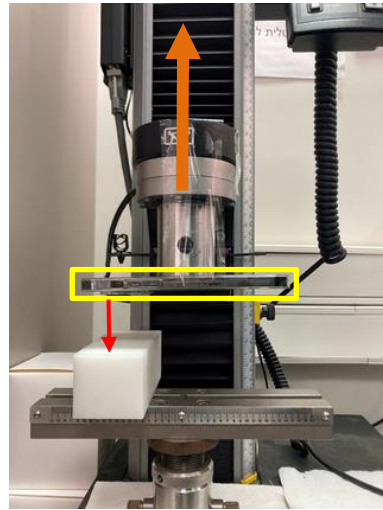


Figure 8 - The calibration system using Instron machine and iPhone Pro's LiDAR sensor. The tapped iPhone is marked in yellow, the red arrow refers to the LiDAR beam direction towards the white box below and the orange arrow refer to the direction in which the system moved during the test.

Secondly, the pre-defined parameters were set as described in Table 1, so that the distance between the LiDAR sensor and the box was measured using a ruler and the steady velocity in which the Instron moved during the measurement was set as well. The accuracy evaluation of the iPhone Pro LiDAR sensor using material testing machine (Instron) was included five different sets of measurements. The initial parameters were described in Table 1.

Table 1 - The initial parameters of the calibration measurements

Tests sets	Initial distance [mm]	Velocity that was set in the machine [mm/min]
1	210	75
2	210	75
3	210	100
4	370	100
5	370	100

Then, the LiDAR sensors started recording at the same time the Instron machine started to move upwards in a steady velocity as defined in advanced in the corresponding SW. During the measurement it was ensured that the LiDAR sensor beam is directing towards the white box in the entire measurement and doesn't direct to any other surface as the distance between the sensor and the box increased. When the machine stopped, the measurement by the LiDAR stopped as well and the data of both the distance and the velocity during the measurement was extracted to Excel file from the two different measurement methods (i.e the Instron and the iPhone). The data obtained from the two distinct instruments were gathered and subsequently analyzed using the MATLAB software (Appendix 9.3).

4.2.2 Design a new method for motion capture system

In order to enable the LiDAR sensor system to accurately track a person's StS movement, a wearable belt system was specifically designed, to securely hold the iPhones, ensuring precise and stable measurements. The wearable belt was designed to ensure that it does not disrupt the ability to perform the StS movement. Emphasis was placed on creating a design that prioritizes comfort, simplicity, and ease of both wearing and using the device. This careful consideration was particularly important as the system is intended for use by older individuals and people with mobility difficulties.

The belt system was ingeniously designed to position the LiDAR sensor in close proximity to the user's Center of Mass (CoM), ensuring accurate measurements while accommodating users of various sizes. To achieve this, two adjustable belts were utilized, integrating stands to securely hold the two iPhones. One device was positioned on the subject's back with the sensor facing upwards, while the other device was situated on the subject's front, orienting the sensor towards a wall in front. Additionally, a belly belt was introduced atop the belt system to ensure stable movement without vibration. The entire belt system is demonstrated in Figure 9.

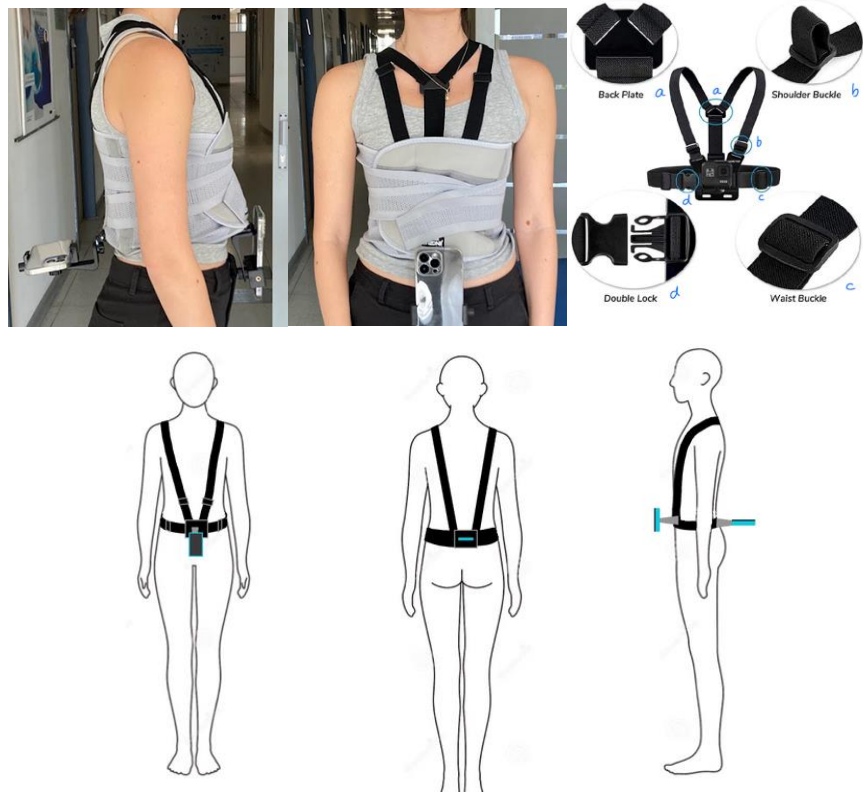


Figure 9 - Demonstration of the wearable belt system with iPhone mounts and belly belt for improved stability

In addition, an upper surface was assembled to ensure a measurement below 5 meters between the iPhone on the back and the surface it's directing and a conventional table chair without back support was used as the sitting base, as demonstrated in Figure 10.



Figure 10 - Demonstration of the upper surface used for the experiment

Additionally, MI SMART SCALE digital weight was employed to measures the subject's weight in various positions; standing, sitting without SnS device, and sitting with SnS device.

4.3 The Experimental Protocol

4.3.1 The Experimental Setup

Before performing the experiment, a few preparation steps should have been performed. First, the chair should have been placed on a flat and horizontal surface in front of a straight blank wall, and be arranged so that the subject sitting with his face directing towards the wall. The horizontal distance between the proximal edge of the chair's seat and the wall required to be within the range of 1-3 meters, and the overall distance of the iPhone LiDAR sensor from the surfaces in both directions had to be kept within the range of 10cm to 5m during all the subjects' movements in the experimental sessions. Additionally, during the recording it was important to ensure no objects (other than those described in this protocol) are placed in between the chair and the wall. In order to ensure proper position of the belt system to the subject, the adjustable strap should have been worn tightly on the subject's torso with the phone mounts placed as close as possible to the Center of Mass (CoM) of the subject. The CoM of subjects is approximated to be an inch below the navel along the centerline of the body [38]. In addition, a belly belt added to maintain the stability of the system. Additionally, the smartphones should have been placed and secured in the phone mounts and the "Physics Toolbox Sensor Suite" application opened. On the smartphone, under "Kinematics", the "Motion Visualizer" button clicked, and then, from the bottom menu the "chart" button was chosen (Figure 11).



Figure 11 - “Physics Toolbox Sensor Suite” application screens

4.3.2 StS maneuver without using the SnS device

4.3.2.1 Initial steps before recording

First, the subject performed **Pre-Initial Sitting Posture (PSP)**; the subject shall sit comfortably on the chair while their legs are placed on the ground and face the wall.

Next, the subjects moved to the **Initial Sitting Posture (ISP)**; before starting the StS Manoeuvre, the subject shall prepare to stand, with both legs placed on the ground and face the wall. The back and neck of the subject should be as straight as possible. The feet of the subject should be approximately a shoulder span apart, fully touching the ground such that the ankles are placed in the instructed StS strategy (Figure 12).

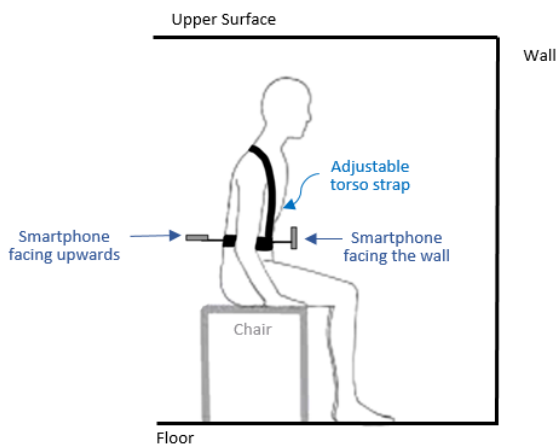


Figure 12 - Demonstration of the ISP; the subject is sitting on the chair, facing the wall, while both legs are placed on the floor.

Then, the subject should practice (one time) the **StS maneuver**, i.e., the subject should lean forward, thereby slightly moving their weight to the front of their feet until reaching full standing position, hands shall be crossed over the trunk.

In the next step, a few measurements should be documented as follows: The subject's body weight while standing, the subject's legs-weight while sitting on the chair and the subject's legs-position distance from the chair's front-legs (BoS). The measuring process should be as such that the subject's legs are positioned on top of the scale for the three different postures described. For the standing measurement, the subject should stand while all of his weight applied on his feet and so his entire weight was measured by the scale. On the other hand, in the sitting postures, the subject should be seated on a standard chair with or without the SnS device on top of it, while his feet are on the scale, so the weight that is being measured by the scale is the part of the subject's weight that applied on his feet while the rest of his weight does not consider in the scale measurement. By this calculation, it is possible to evaluate the change in the CoM position during standing movement and demonstrate how the subject's weight distribution differs when sitting on a standard chair in compare to using the SnS device.

4.3.2.2 Experimental flow

The experiment itself starts when the subject sits comfortably in the PSP (as explained previously) with the smartphones well secured in the mounts and the LiDAR sensors' beams projection areas are clear from any obstructions while they are facing the wall and the upper surface. Then, the "Record" button shell be clicked in the "Physics Toolbox Sensor Suite" application (a notification will appear, indicating that data recording started). After 10 seconds of waiting in the standing position the subject shall sit in the ISP position (as described earlier). Next, the subject shall perform the StS maneuver (as explained in the initial steps). Another 10 seconds of waiting shell be performed before and after the subject sit back on the chair. This sequence of steps shell be repeated three times and then the "Stop" button shell be clicked in the "Physics Toolbox Sensor Suite" application to stop the recording. After the recording has stopped, the recording's data shell be immediately exported by choosing the relevant option suggested by the application (for example, export to email, Google Drive etc.). In the experiment carried out,

the recording was continuous throughout all the repetitions, so that the transition from standing to sitting was also recorded.

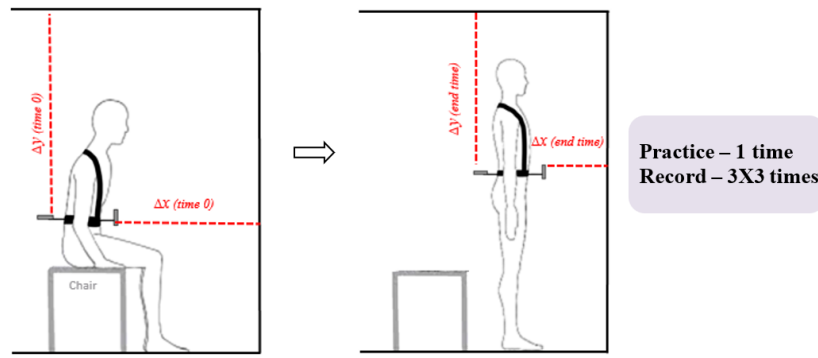


Figure 13 - Demonstration of StS maneuver without the support of the SnS device; the subject is performing the StS maneuver while facing the wall. The distance from the wall as well as the distance from the upper surface are being recorded.

4.3.3 StS maneuver with the support of the SnS device

4.3.3.1 Initial steps before recording

First, the SnS device shell be taken out of the case and be placed on the chair while it is deflated, as being shown in Figure 14.



Figure 14 - SnS device is placed on the chair so that the inflatable cushion is on the seat while deflated

Then, the subject shall practice (one time) the **StS maneuver while using the SnS** ('StS -SnS maneuver), i.e., to perform the StS maneuver, while the subject inflates the four SnS cells to the fully inflation stage with the controller, until the subject reaches a full standing position. The subject should perform the StS -SnS maneuver while hands are crossed over the trunk.

4.3.3.2 Experimental flow

The experimental flow while using the SnS ('StS -SnS maneuver) is equal to the flow described for the measurement without using SnS device (section 4.3.2) but with using SnS device (Figure 15).

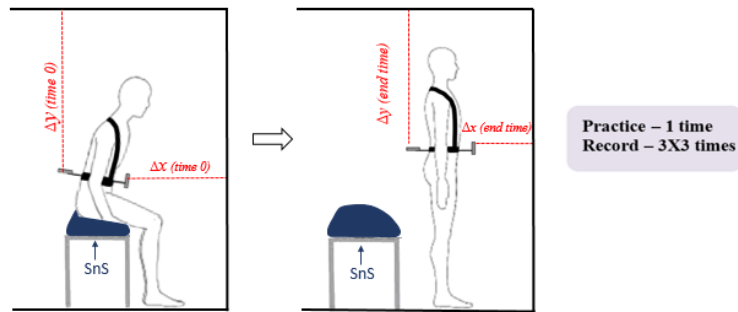


Figure 15 - Demonstration of StS maneuver with the support of the SnS device; the subject is performing the StS maneuver using the SnS ('StS -SnS maneuver') while facing the wall. The distance from the wall as well as the distance from the upper surface are being recorded

4.4 Outcome Measures

In order to evaluate the safety and effectiveness of the SnS device in reducing the risks associated with rising from a chair, equations (1)-(7), outlined in chapter 4.1, were computed separately for each section of the StS process.

The comparison was evaluated between the results obtained with and without the SnS device for the same subject at the same axis (i.e x axis; for the measurement of the subject's CoM distance from the wall in front and y axis; for the measurement of the subject's CoM distance from the upper surface on top).

4.4.1 Signal Processing

The first step of the results analysis included the processing of the position signals extracted from the "Physics Toolbox Sensor Suite" application. Each recording that extracted from the application, for each experimental subject, included the three repetitions of Sit-to-Stand and Stand-to-Sit together with the standing and sitting periods between them. Hence it was necessary to process the recordings and extract only the three repetitions of Sit-to-Stand each examinee conducted. Accordingly, a MATLAB code (Appendix 9.4.1) was created which extracted the sequences within the recordings where the StS was performed. The method of StS sections extraction was as such; the derivative of every LiDAR signal was calculated

and whenever the derivative was above 1 it indicated of StS section (the slopes of the other sections were within a range of 0 to 0.976).

The second step was to reduce from each signal the last distance recorded for the StS section. The standing point was defined as the reference point, so the motion that was evaluated was the difference between the CoM position during the StS motion to the standing (i.e. ending point) of the motion.

4.4.2 Statistical Analysis

The next step of the evaluation was computation of statistical measurements in order to evaluate whether there is a significant difference between the StS movement with the SnS device compared to the StS movement without it. Therefore, the p-value of one-way ANOVA test was calculated between the 2 sets of 3 signals repetitions of each subject with and without the assistance of the SnS device. So that the computational measurements (as described in section 4.1) were applied on each of the signals so that the difference between the equation's outcomes were evaluated using ANOVA test in the same way, by the built-in MATLAB function “anova1” (Appendix 9.4.2). Next, in order to determine which equation is capable of significantly distinguishing between StS movement that conducted with the SnS device and without it, the number of tests of each measurement that was found significantly different ($p_{value} \leq 0.05$) was counted, to assess whether most of the p-value results obtained for the different subjects were significant or not. In addition, the ANOVA test was also computed on the 2 sets of StS position signals repetitions each examinee conducted in an attempt to consider if there was a significant difference between the movements themselves, in the sense of understanding whether there was any difference between the movements before applying and assessing the computational assumptions.

Furthermore, the average of the results obtained from the equations for each set, which includes three sections of the StS movement, was computed. Subsequently, the relative difference in measurements between the sections with and without the utilization of the SnS device was calculated for each subject according to the following equations:

$$\text{Eq. 7} \quad \text{relative difference(axis)}_{q,i} = \frac{\text{average}_{\text{without}} - \text{average}_{\text{with}}}{\text{average}_{\text{without}}} \cdot 100\%$$

Where $q.i$ refers to the computational model's assumption, with refers to the average of the measurement with the SnS device and without refers to the average of the measurement without the use of SnS device

In this calculation, the absolute value was disregarded. This was done to indicate the direction of the difference, so that when the results are positive, it implies that the results obtained from the computational assumption, for the StS action with the assistance of the SnS device, were lower than those obtained for the StS action without the use of SnS. Accordingly, positive results would indicate a correspondence to the expectations, as we aspire to receive minimal results for the equations of the measurements were taken with the use of the SnS device. Ultimately, the average of all the relative differences was calculated.

These operations were performed for each equation between each pair of relevant sets, considering the same axis, both with and without SnS, for each subject.

Moreover, the duration of time it took for each subject to perform StS movement with and without the SnS was measured and compared.

A few calculations made for the evaluation of the weight measurements while sitting on a chair with and without the SnS device, as follows:

$$\text{Eq. 8} \quad \text{Relative Normalized Difference} = \frac{\text{Weight}_{\text{with SnS}} - \text{Weight}_{\text{without SnS}}}{\text{Total standing weight}}.$$

100 [%]

$$\text{Eq. 9} \quad \text{Ratio} = \frac{\text{Weight with SnS}}{\text{Weight without SnS}}$$

4.4.3 Qualitative Analysis

The purpose of the qualitative analysis that would be describe in this section is to provide another insight to the results from the visual appearance that was analyzed using the video recordings that were taken during the experiments. First, plots were drawn based on the extracted segments (Appendix 0), whereas the qualitative analysis was performed by comparing those plots to the video recordings of the StS Movement during the experiments. The comparison of the graphs to the video recordings enable us to better understand the patterns appeared on the graphs and find a proper explanation for them. That is to identify normal and abnormal patterns (per subject) to assess whether the movement conducted by the subject was stable or unstable and whether we can extract identifiers for instability while performing StS with and without the assistance of the SnS.

Also, models that describe the typical StS movement with and without the SnS were created, based on the 8 participants analyzed in the experiment, using the LiDAR sensor in the two axes. The models were based on the average measurement of the position signal for each sample over the recording time-period at the StS sections.

Similarly, average models of StS Movement using SnS device were generated and compared to the previous averaged models.

5 Results

5.1 Calibration of the LiDAR sensors

The accuracy's evaluating of the iPhone Pro LiDAR sensor using material testing machine (Instron) was included five different sets of measurements. The initial parameters were described in Table 2.

Table 2 - The initial parameters of the calibration measurements

Tests sets	Initial distance [mm]	Velocity that was set in the machine [mm/min]
1	210	75
2	210	75
3	210	100
4	370	100
5	370	100

The results obtained from the two devices were compared by calculating the following errors (Table 3) as well as by plotting them on corresponding graphs (Figure 16-Figure 20).

Table 3 - The position errors between the two devices

Tests sets	STD [mm]	mean square error [mm]
1	37.86	4.19
2	201.49	8.67
3	48.40	2.50
4	22.74	1.57
5	27.47	3.96

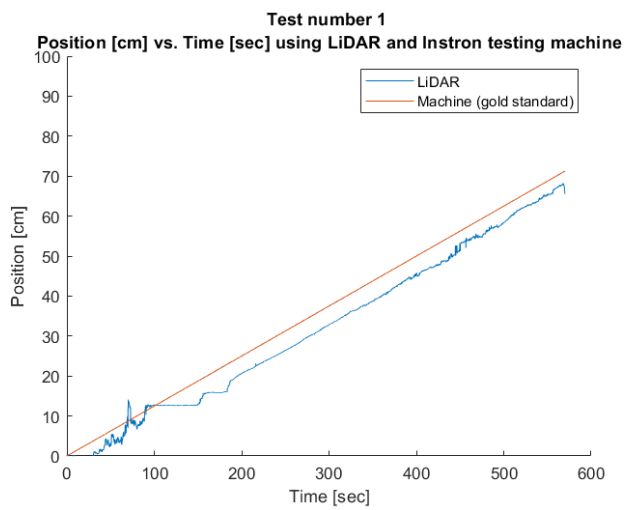


Figure 16 - Calibration result of set 1. LiDAR-blue graph, Machine – orange graph

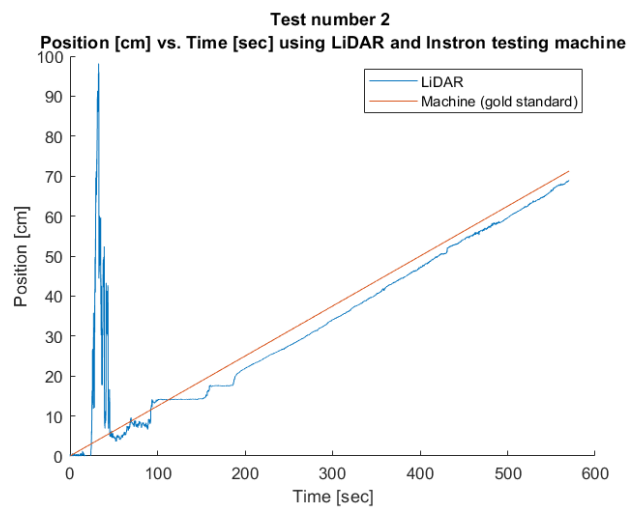


Figure 17 - Calibration result of set 2. LiDAR-blue graph, Machine – orange graph

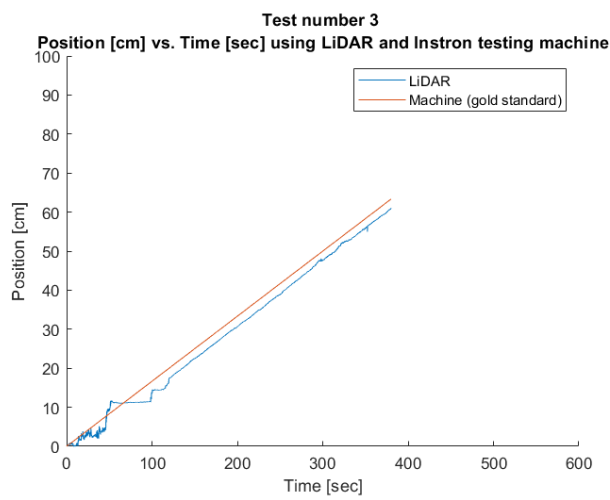


Figure 18 - Calibration result of set 3. LiDAR-blue graph, Machine – orange graph

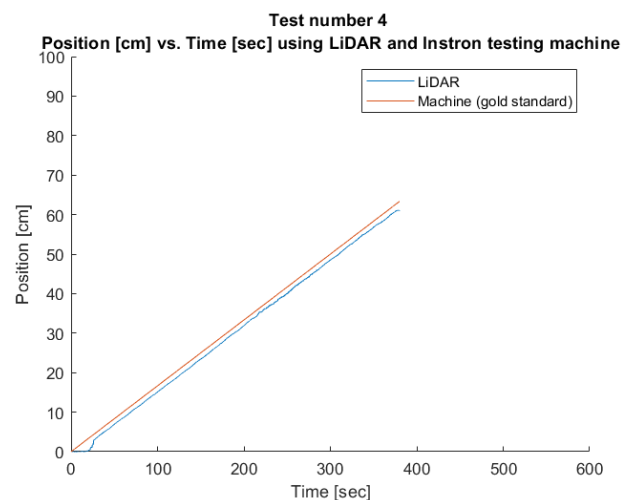
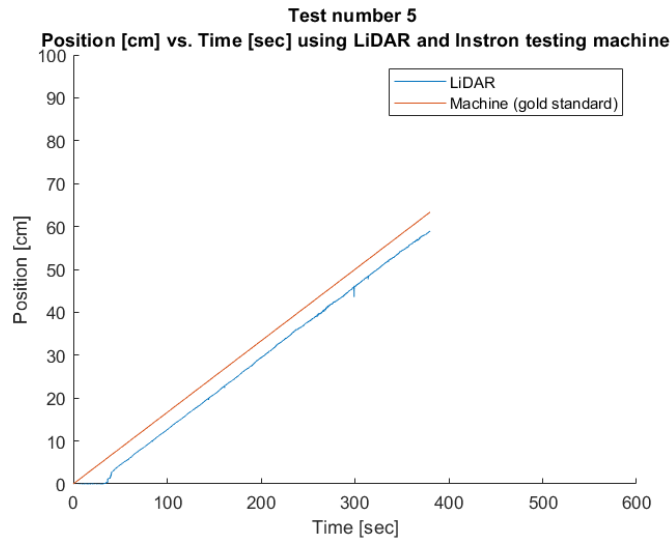


Figure 19 - Calibration result of set 4. LiDAR-blue graph, Machine – orange graph



**Figure 20 - Calibration result of set 5. LiDAR-blue graph,
Machine – orange graph**

As can be seen, the LiDAR measurement accuracy improved as the initial distance from the surface increased and the STD were lower as well. Although, the percentages of mean square errors are still quite high (higher than 5%) and showing a difficulty of the LiDAR to measure accurately the distance of the phone from the target surface. Despite this drawback, the LiDAR has acceptable measurement of the movement and because the evaluation of the movement in this project were measured relatively the LiDAR's measurement ability satisfies the experimental requirements for evaluating the StS movement. In addition, it is important to note that the calibration was conducted in range of distances that were not adequate to the recommended measurement for best accuracy, while the measurement during the experiments was conducted in a range which defined accurate according to the device's specifications.

5.2 1st Experiment Session Results

All Trial 1 experiments were done while the SnS inflated only up to level 2 (out of 4) due to device malfunction.

5.2.1 Information regarding the Experimental Participants

8 adults (3 females, 5 males), in a range of 63-72 years old were participated in the experiment. 3 Subjects noted that they suffer from a certain medical condition that may

affect the StS Movement. However, most of the adults reported that they have no difficulty performing StS daily. Below (Table 4) is a summary of the relevant personal and physiological details about the Subjects.

Table 4 - Personal and Physiological details about the Subject

Subject	Gender	Age [year]	High [cm]	Wight (standing) [kg]	Notes	Difficulty performing StS *
1	Female	67	145	44		0
2	Female	63	145	50.45		0
3	Male	70	170	80.8		0
4	Male	69	168	78.4		0
5	Female	66	151	54.55	Suffers from Osteoporosis	1
6	Male	67	170	90.9	Experienced instability events in the Last year (dizziness and fall)	1
7	Male	72	172	79	Had a knee joint replacement this year	1
8	Male	63	170	68.8		0

* The subjects were asked to indicate if there is any difficulty in performing StS, as follows:

0 - no difficulty, 1 – light difficulty, 2 - moderate difficulty, 3 - significant difficulty, 4 - cannot be performed without external help

5.2.2 The SnS device effect on the CoM position

The subjects' weight was measured in three situations: standing, sitting without SnS device, and sitting with SnS device. The results are shown for the 8 subjects in Figure 21.

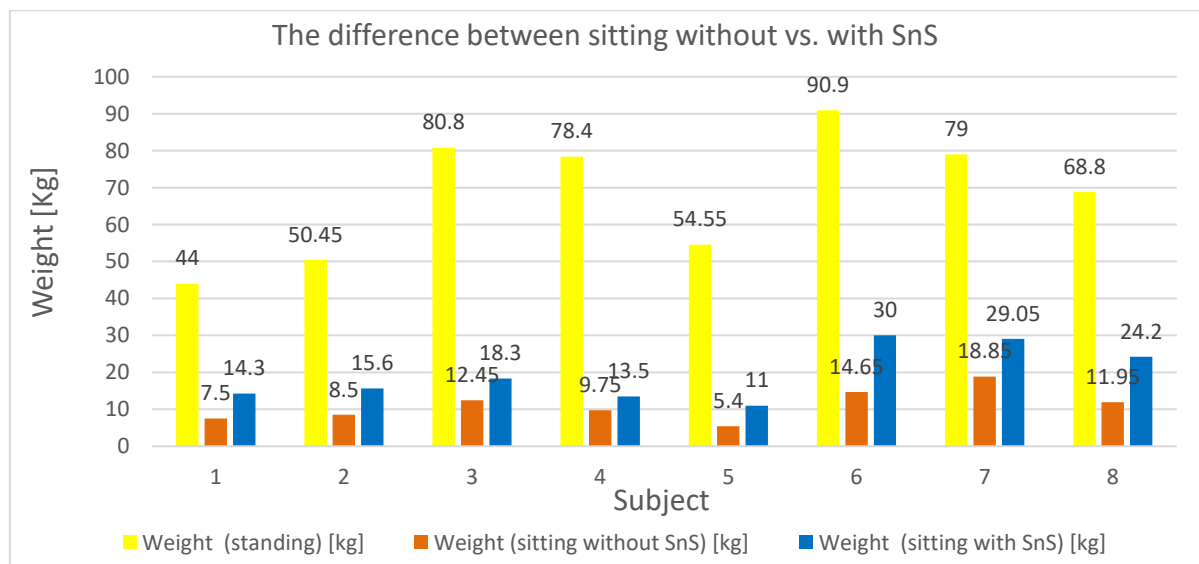


Figure 21 – bar graph that compares the weight measured while sitting with and without the SnS device for each of the subjects

As it appears from the measurement results in Figure 21, for each of the experimental subjects, the weight while sitting on the SnS device was higher than without in, so that the use of SnS device almost doubled the body weight with an average ratio of 1.781 ± 0.274 and averaged difference of 8.36 ± 3.9 Kg between the sitting position. For the females, who were all up to 155 cm height, the average ratio was 1.926 ± 0.231 , and for the male, who were all above to 155 cm, the average ratio was 1.694 ± 0.284 . Additionally, the averaged relative normalized difference between the weight measured while sitting with the SnS and without it was $12.4 \pm 4.6\%$.

5.2.3 Modeling StS maneuver

As can be seen in the attached plots in Figure 22 and Figure 23, that present the signals of StS movement without assistance that collected from each subject using the LiDAR system, as well as the average of the signals, there are unique characteristics that define the StS Movement in x and y axes.

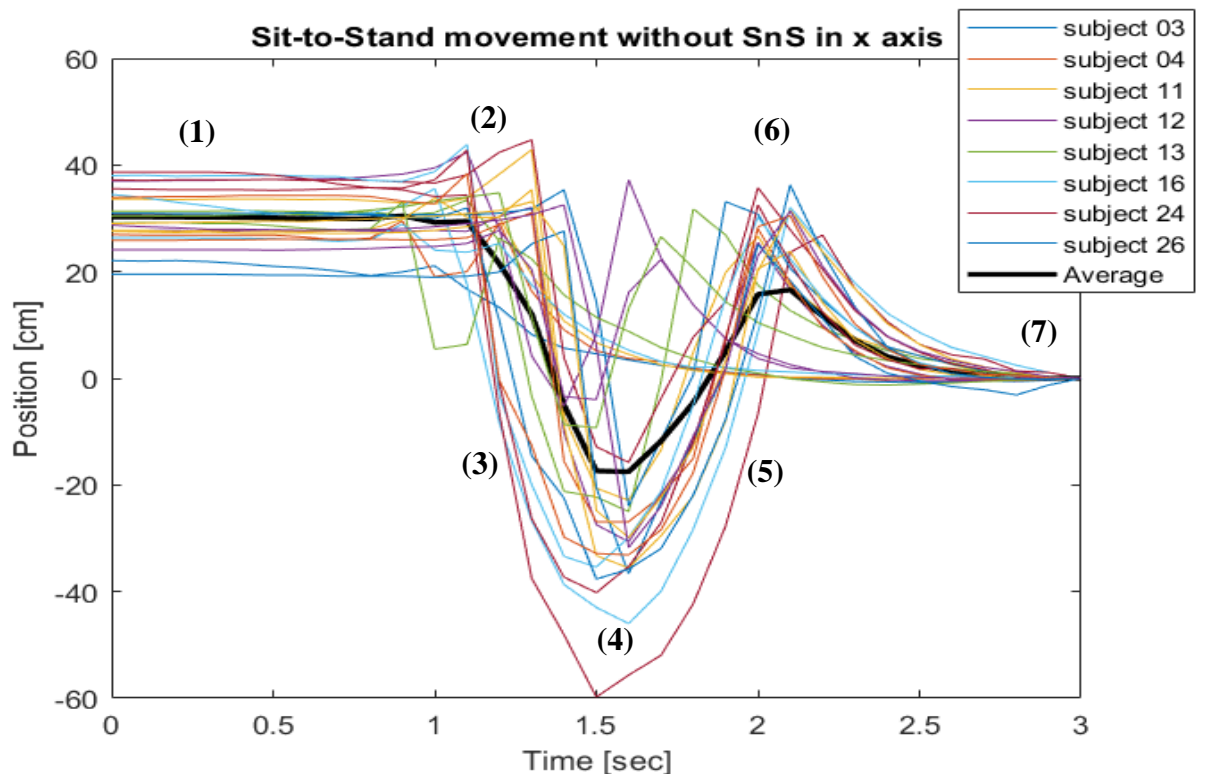


Figure 22 - Model of StS movement of x axis (colorful – all the subjects' measurements, black – the weighted average model)

As it appears in Figure 22, there was an overall similar trend of the StS movement performed in x-axis for each of the different subject. The movement in x-axis includes the following characteristics; First a steady line started the recording (1). Then, at the beginning of the seat-off, a light upward peak called "positive peak" (2) can be recognized. Afterwards, a sharp downward slope (3) that ends in a dominant downward peak called "negative peak" (4) around 1.5 second from the beginning of the recording. Then an upwards slope appears in the graph (5) and right after the negative peak section ends, another light positive peak (6) is recognized and right afterwards the steady line appears (7). In addition, as can be seen in Figure 60 and in Appendix 9.1 (per subject analysis) the movement in x axis was consistent.

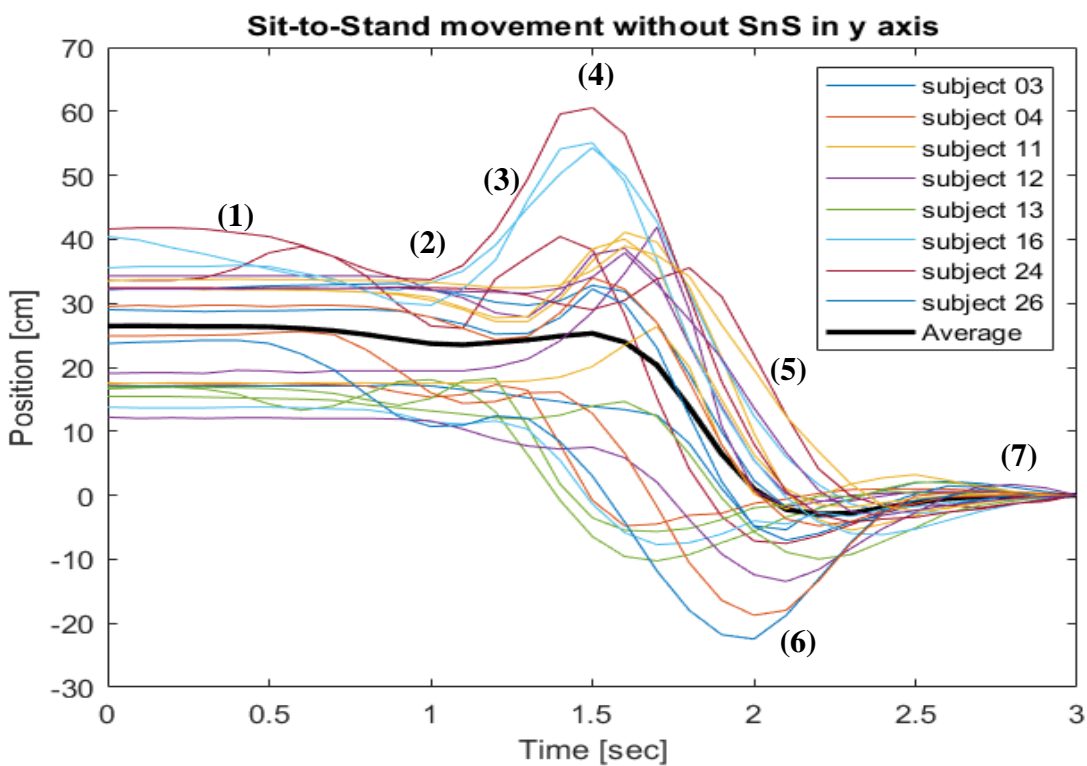


Figure 23 - Model of StS movement of y axis (colorful – all the Subjects' measurements, black – the weighted average model)

As it appears in Figure 23, the movement in y-axis included the following characteristics; First a steady line started the recording (1). Then, at the beginning of the seat-off, a light downward peak called "negative peak" (2) can be recognized. Afterwards, a

light upwards slope (3) that ended in an upward peak called “positive peak” (4) around 1.5 second from the beginning of the recording can be seen. Next, a dominant slope downwards appeared (5), another light negative peak (6) was recognized and right afterwards the steady line was appeared (7). In addition, as can be seen in Figure 61 and also in appendix 9.1 (per subject analysis) the movement in y axis was consistent.

The same process was done for the recordings of the StS performed with the SnS device and results of the models generated are present in Appendix 9.2.

5.2.3.1 Statistical Analysis results

Table 5 displays the p-values, which calculated, using ANOVA test, between the results of the computational assumptions (formula (1)-(6)), with and without using SnS device for each subject, divided into x and y axes. In addition, the success rates which describe the significant p-values percentage of each computational assumption (*p value < 0.05*), divided into the axes, presented in the bottom of the table.

Table 5 - p value for all the computational assumptions per subject

(The significant results were marked blue)

Subject	X axis				Y axis			
	AUC [cm·sec]	Velocity [cm/sec]	Acceleration [cm/sec ²]	Position [cm]	AUC [cm·sec]	Velocity [cm/sec]	Acceleration [cm/sec ²]	Position [cm]
1	0.03	0.71	1.00	0.01	0.21	0.78	0.99	0.59
2	0.36	0.63	1.00	0.08	p<<0.05	0.88	0.99	p<<0.05
3	0.14	0.89	1.00	0.15	0.75	0.64	0.96	p<<0.05
4	0.77	0.98	0.99	0.57	0.96	0.69	0.98	0.80
5	0.20	0.83	0.99	0.03	0.81	0.97	0.96	0.08
6	0.07	0.90	1.00	0.02	0.01	0.74	0.94	p<<0.05
7	0.02	1.00	1.00	0.05	0.70	0.90	0.97	0.10
8	0.69	0.94	0.99	0.07	0.17	0.51	0.97	0.01
Success rate [%]	25	0	0	50	25	0	0	50

First, as it clearly appears from Table 5 above, there was a correspondence between the axes as the success rates were identical for the two axes. Also, the highest success rate for significance difference between the StS movements obtained from the signals themselves, which present in the table as “Position”, with a success rate of 50% between the 8 subjects examined, in both axes. The area under the curve (AUC) was the most promising computational assumption, out of the three assumptions used in this project to evaluate stable and safe StS motion, with success rate of 25% for both axes. The two other computational assumptions couldn't indicate for significant difference between the StS movements with and without the SnS.

Table 6 - The difference [%] of all the computation assumptions per subject in each state

(The positive relative difference results were marked in green)

Subject	X axis			Y axis		
	AUC [cm·sec]	Velocity [cm/sec]	Acceleration [cm/sec ²]	AUC [cm·sec]	Velocity [cm/sec]	Acceleration [cm/sec ²]
1	-6.56	-20.94	-45.32	-0.67	-39.63	-43.37
2	-1.19	-66.85	-36.14	-3.09	-200.56	-184.61
3	1.96	8.35	23.62	1.91	-33.53	-39.83
4	-5.57	8.70	14.76	1.71	3.10	-1.03
5	0.74	-12.63	-2.85	1.65	-11.57	-37.55
6	-8.71	25.34	1.76	4.80	30.80	9.51
7	-5.51	18.91	13.67	3.32	19.92	25.31
8	0.77	28.55	19.60	3.20	12.69	5.02
Success rate [%]	37.5	25	75	75	37.5	87.5

Table 6 presents the relative difference values (Eq. 7), which calculated between the average results of each computational assumption, with and without SnS device, divided into x and y axes. Additionally, the percentage of the positive relative difference was measured for each computational assumption at the two axes, refer as success rate.

As the table shows, the success rates were higher in the y-axis in compare to x-axis for each of the computational assumptions respectively. Also, when looking on each subject separately, it can be recognized that both 3 and 4 subjects received only negative relative differences for all of the parameters that were measured, while in contrast, all the

relative differences were positive for subject 8, indicating that there was a variation between the subjects that influenced the effect of the SnS device success. In addition, as it appears, the success rate was the highest for the Acceleration in both axes, right afterwards the AUC measurement received the next highest rate and at last, the Velocity had the lowest rates.

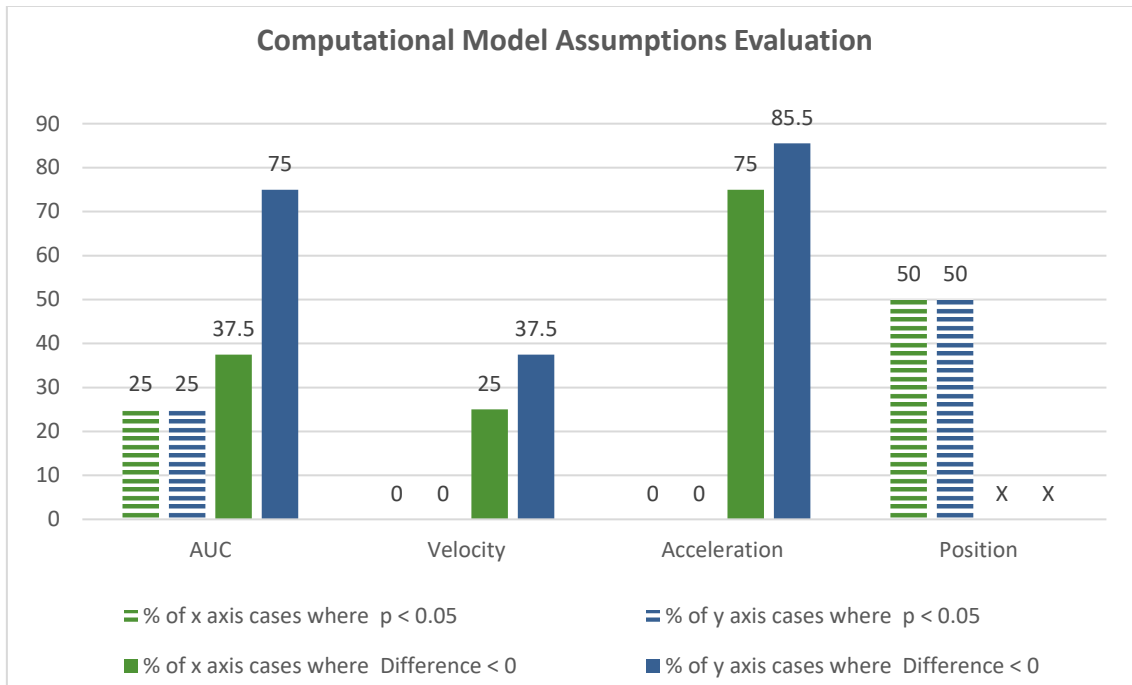


Figure 24 - bar graph that summarizes the success rate of the statistical results measured [p-value<0.05 from ANOVA test & relative difference<0] for each computational model parameter [AUC, Velocity, Acceleration, Position]

The bar graph on Figure 24 summarize the success rates that were shown in Table 5 and Table 7 which discussed previously, in order to visually express the outcomes obtained from the statistical calculations.

In addition, the duration of time it took for each experimental subject to perform the StS movement was measured and compared when conducted with the assistance of the SnS device and without it. The average results of the measurements are presented in Table 7 below:

Table 7 - StS Duration of time with and without SnS in x and y axes

x axis	y axis

Without SnS [sec]	With SnS [sec]	Without SnS [sec]	With SnS [sec]
2.9	2.79	2.91	2.79

As Table 8 display, in both axes, the duration of time to perform StS was higher without the SnS, with a relative difference of 4%.

5.2.4 Evaluation of the SnS Device's Effect by the Models

Based on the averaged results obtained while performing StS Maneuver using SnS device (as can be seen in Appendix 9.2) and without assistance (as can be seen earlier in Figure 22 and Figure 23), in both axes, the models in Figure 27 below were formulated. These models are shown together in order to enhance the similarities as well as the distinctions that can be seen when comparing the structure of the StS movement in the two options, i.e. with and without the use of SnS device. Additionally, Figure 25 and Figure 26 demonstrate the directions of the LiDAR's beam during the StS movement with and without the use of SnS device respectively and serve explanations to the characteristics of the models and the cause for the variations between the differences appeared in the graphs.



Figure 25 - The LiDAR beam directions during StS movement without the SnS



Figure 26 - The LiDAR beam directions during StS movement with the SnS

Upon examining Figure 25 and Figure 26 above, it becomes evident that there are some notable differences in the orientations of the LiDAR's beams during the StS task with and without the SnS. Specifically, when focusing on the "Sitting" image, it is apparent that the subject's body position on the chair differs between the conditions with and

without the SnS. With the SnS, the subject leans back, causing the LiDAR's beam to be directed towards the front wall at a certain angle rather than vertically as observed without the SnS. Consequently, the measured distance by the LiDAR when the subject is seated on the SnS is greater.

Moving on to the "Leaning Over" stage, the LiDAR's beam is directed towards the floor in both cases. However, when the subject rises from the chair without the SnS, the extent of leaning over is more pronounced, resulting in the LiDAR's beam being positioned between the subject's legs. On the other hand, when using the SnS, the leaning over extent is more moderate.

At the end, the "Standing" stage in both cases seems quite similar.

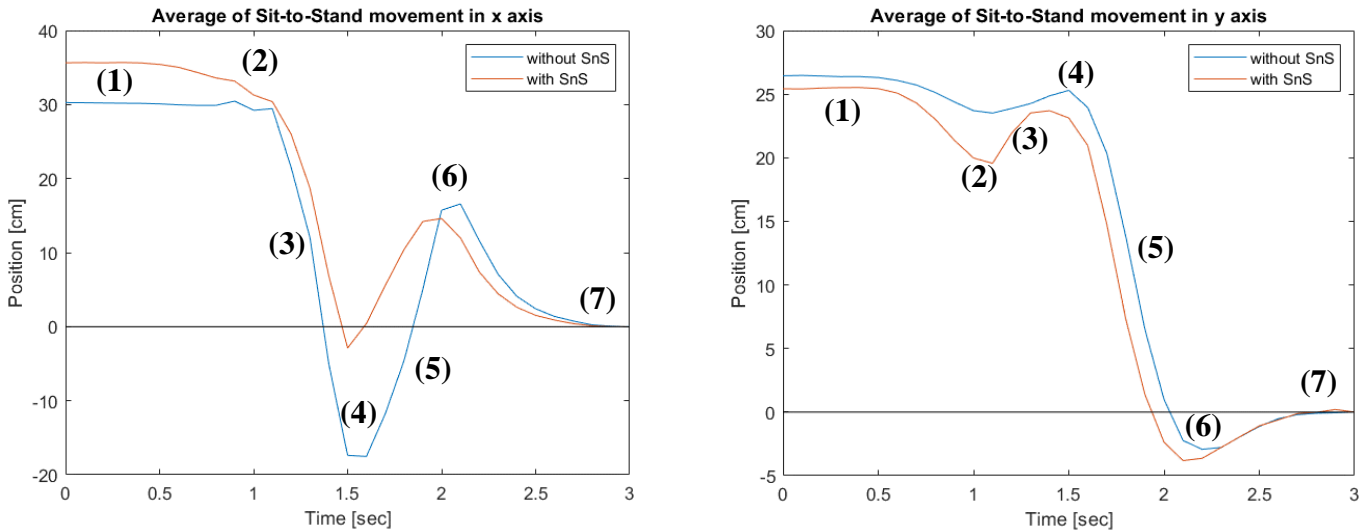


Figure 27 - Model of StS movement without using SnS device of x-axis (left) and x-axis (right). Orange – without using SnS device, Blue – using SnS device

The starting point (sitting, (1)) is different in both cases and on both axes, whereas the difference in x-axis is greater than the difference in y-axis. Additionally, as it appears, while on x-axis the averaged position is higher when using SnS, on the y-axis the opposite phenomenon observed so that the position is higher in the starting point when conducting StS without the SnS device. In contrast, at the end point (standing, (7)) there is no difference between positions with and without SnS and that is because the ending point was reduced from each signal as described earlier in section 4.4.1. Moreover, each graph is characterized by 3 peaks ((2), (4), (6)), where the peaks of x-axis correspond to the peaks

of the y-axis in the opposite way (a negative peak in one axis found positive on the other, and vice versa), both with and without using SnS device. Out of the two less dominant peaks ((2), (6)), peak (2) represents the preparation phase for seat off, and is less dominant than peak (6) on x-axis, and on y-axis the situation is reversed, in both cases. This accompanied by the degree of the slopes ((3), (5)) in a similar trend, where on x-axis there is a slope (3), which represents the seat off phase more dramatically than y-axis, in both cases. Besides, in both cases the most dominant peak is (4).

Beyond that, on x-axis the average model obtained using SnS device is mostly above the model without using SnS device, while on y-axis the situation is reversed.

Further, based on the analysis conducted per subject (appendix 9.1), when comparing the graphs with and without SnS in y-axis to those in x-axis, it appears, visually, that it's easier to distinguish between the graphs with or without the SnS on y-axis in compared to x-axis.

5.3 2nd Experiment Session Results (Post Protocol Improvements)

Due to a malfunction in the inflation of the SnS during the first experimental session, a subsequent session was conducted with several additional adaptations. These adaptations aimed to address the issue and ensure more accurate measurements. Firstly, participants were instructed to straighten their backs as much as possible during the StS movement. This instruction aimed to enhance the detectability of signal variations caused by different torso angles, thereby improving measurement accuracy.

Secondly, a marking was placed on the chair to indicate the specific location where participants should sit for all experimental repetitions, both with and without the SnS. This step was taken to eliminate the potential impact of variations in seating position on the analysis of signal differences. By maintaining consistent seating positions throughout the experiment, the influence of positional discrepancies on signal analysis was minimized.

5.3.1 Information regarding the Experimental Participants

The participants of the 2nd trial of the experiment were 3 women in a range of 26-35 years old, who have no difficulty in performing StS action on a daily basis, which

performed the experiment with the additional instructions added to the experimental protocol as previously described.

5.3.2 The SnS device effect on the CoM position

The subjects' weight was measured in three situations: standing, sitting without SnS device, and sitting with SnS device. The results are shown for the 3 subjects (A, B, C) in Error! Reference source not found..

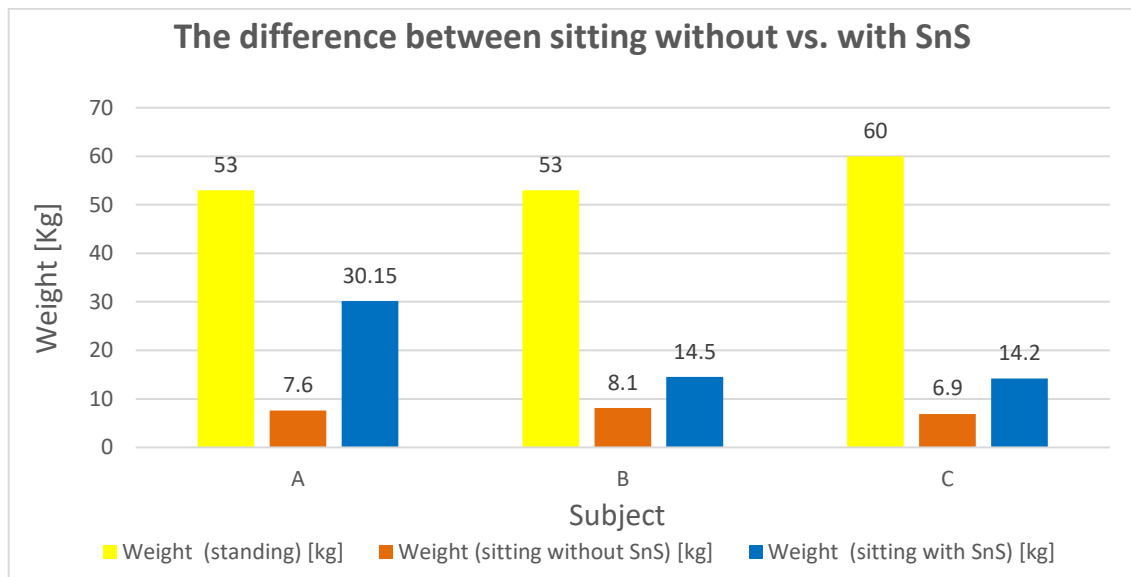


Figure 28 - bar graph that compares the weight measured while sitting with and without the SnS device for each of the subjects

In correspondence to the results obtained in the 1st experiment trail, as it appears from the graph in Figure 28, for each of the experimental subjects, the weight while sitting on the SnS device was higher than without it, so that the use of SnS device increased the weight applied on the feet with an average ratio of 2.6 ± 1.18 , average normalized difference of $22.26 \pm 17.57\%$ out of the subject's body weight, and an averaged difference of 12.08 ± 9.08 Kg between the sitting position.

5.3.2.1 Visual Evaluation of the SnS Device's Effect on StS

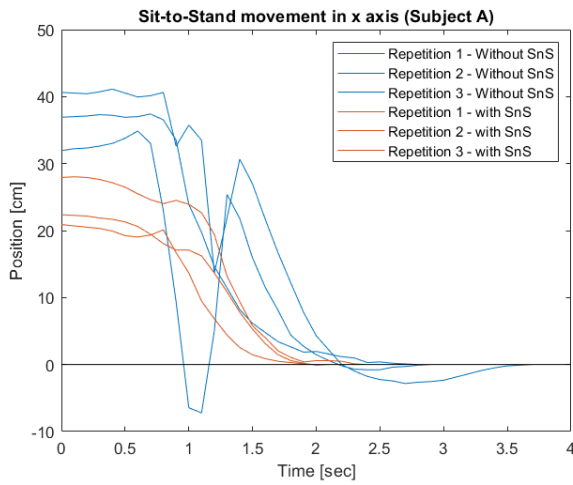


Figure 29 - subject A - StS movement on x axis:3 repetitions without using SnS device (blue); 3 repetitions using SnS device (orange)

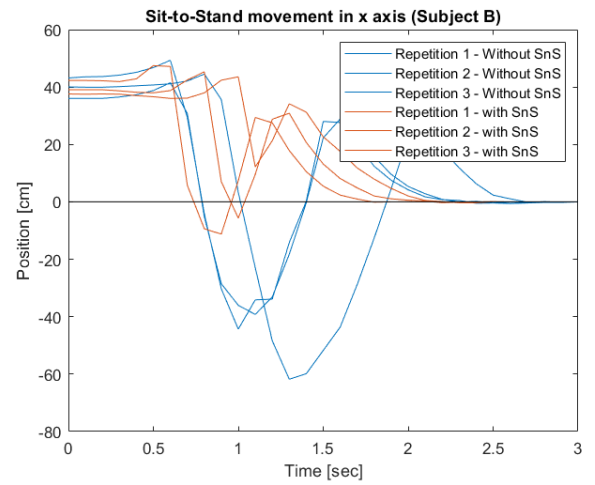


Figure 30 - subject B - StS movement on x axis:3 repetitions without using SnS device (blue); 3 repetitions using SnS device (orange)

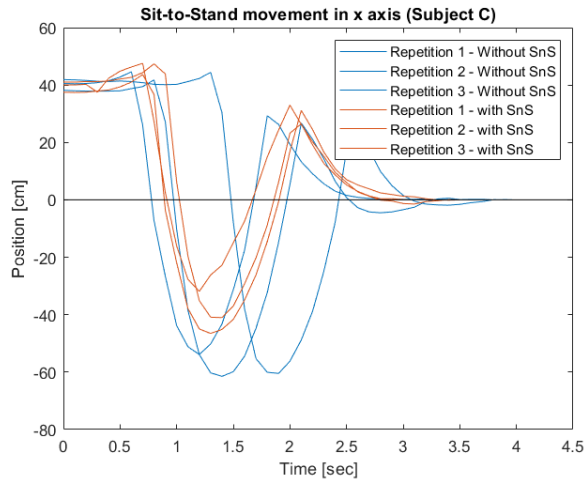


Figure 31 - subject C - StS movement on x axis:3 repetitions without using SnS device (blue); 3 repetitions using SnS device (orange)

As it appears from the graphs on Figure 29, Figure 30 and Figure 31 there is variability between the structures of StS movement that been performed by the different subjects. First, it is most prominent that the movement of subject A was much different from the movements of the other subjects as it's StS with the SnS was a monotonically decreasing signal, and very smooth and repetitive signal, whereas for the other subjects a very dominant negative peak can be seen in the middle of the action. Additionally, when focusing of the movement without the SnS, it is clear that the negative peak appeared on the signals of subject A were more abrupt with high slopes' trends and occurred for a very short time period compared to the motioned recorded for the other participants. Also, the

difference between StS with SnS and without SnS is much easier to visually distinguish compared to the others.

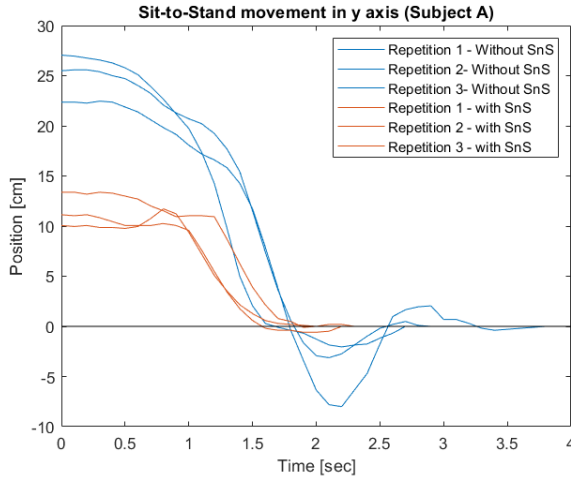


Figure 32 - subject A - StS movement on y axis:3 repetitions without using SnS device (blue); 3 repetitions using SnS device (orange)

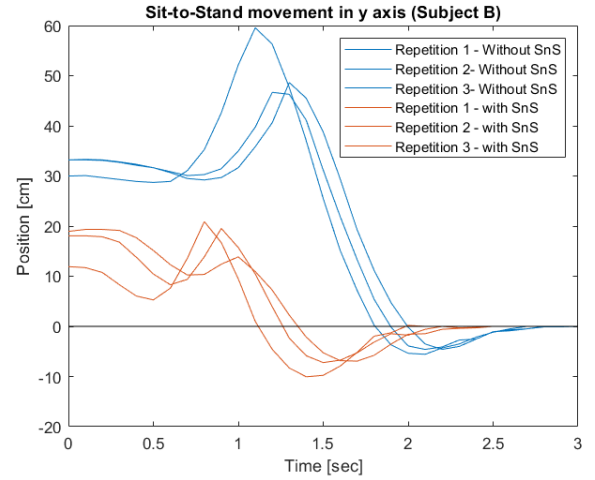


Figure 33 - subject B - StS movement on y axis:3 repetitions without using SnS device (blue); 3 repetitions using SnS device (orange)

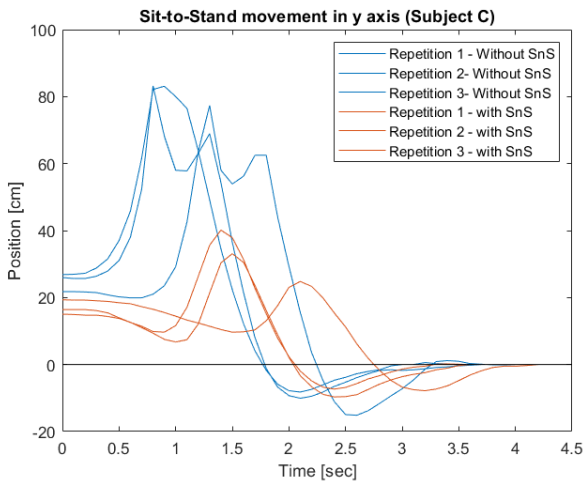


Figure 34 -subject C - StS movement on y axis:3 repetitions without using SnS device (blue); 3 repetitions using SnS device (orange)

In correspondence to what been seen for the x axis, on the graphs on Figure 29, Figure 30 and Figure 31 it is clear that the StS performance of subject A was different than the other examinees of this trial. The most prominent variation that can be recognized is that the movement of subject A both with the SnS and without it was mostly monotonically decreasing signal, and very smooth and repetitive signal, whereas for the other subjects very dominant peaks can be seen along the action.

5.3.2.2 Statistical Analysis results

The statistical results from the 2nd experimental session is presented in the following tables.

Table 8 - The statistical analysis results on x-axis of all the computation assumptions in each state (with and without SnS) for subject A

(The results which support the initial assumptions were marked in green)

		AUC [cm·sec]	Velocity [cm/sec]	Acceleration [cm/sec ²]	StS dura- tion [sec]	ANOVA Between signals
Without SnS	Average	345.4	-8.1	0.0	3.3	-
	STD	23.0	14.0-15.9	58.3-79.9	0.5	-
With SnS	Average	144.8	-5.1	0.1	2.3	-
	STD	26.9	7.7-8.9	44.9-60.3	0.2	-
Difference		58.1	36.5	717.5	28.7	-
<i>p</i> -value		P<0.05	P<0.05	1.0	0.1	P<0.05

Table 9 - The statistical analysis results on x-axis of all the computation assumptions in each state (with and without SnS) for subject B

		AUC [cm·sec]	Velocity [cm/sec]	Acceleration [cm/sec ²]	StS dura- tion [sec]	ANOVA Between signals
Without SnS	Average	649.2	-13.4	0.1	3.1	-
	STD	144.1	1.2	0.7	0.1	-
With SnS	Average	484.5	-16.5	-0.2	2.5	-
	STD	78.1	3.1	0.5	0.3	-
Difference		235.3	-23.4	25.4	17.4	-
<i>p</i> -value		0.3	1.0	1.0	0.1	P<0.05

Table 10 - The statistical analysis results on x-axis of all the computation assumptions in each state (with and without SnS) for subject C

		AUC [cm·sec]	Velocity [cm/sec]	Acceleration [cm/sec ²]	StS duration [sec]	ANOVA Between signals
Without SnS	Average	898.7	-10.4	0.2	4.0	-
	STD	169.4	1.1	0.7	0.2	-
With SnS	Average	726.4	-11.7	-0.1	3.5	-
	STD	61.1	1.4	0.3	0.3	-
Difference		19.2	-12.1	168.3	0.5	-
<i>p</i> -value		0.3	0.3	0.5	0.2	P<0.05

When comparing the statistical results obtained for the three different subjects examined for the experiment, it can be recognized that for all of the examinees the p-value of the ANOVA between the signals were all under 0.05 which means that there was a significant difference between the signals of StS with and without the SnS on x-axis. In contrast, for both B and C subjects, the p-values of all the computational assumptions were higher than 0.05 indicate that there is no significant difference between them. Meanwhile, for subject A both the AUC and Velocity parameters were found significantly different. Regarding the relative difference, it seems as for all of the subjects most of the assumptions had positive values indicating the superiority of the SnS to gain stability. Also, the success rate of the relative difference was the lowest for the Velocity in this experimental trail.

Table 11 - The statistical analysis results on y-axis of all the computation assumptions in each state (with and without SnS) for subject A

		AUC [cm·sec]	Velocity [cm/sec]	Acceleration [cm/sec ²]	StS dura- tion [sec]	ANOVA Between signals
Without SnS	Average	345.4	-8.1	0.0	3.2	-
	STD	23.0	14.0-15.9	58.3-79.9	0.5	-
	Average	144.8	-5.1	0.1	2.3	-

With SnS	STD	26.9	7.7-8.9	44.9-60.3	0.2	-
Difference		58.1	36.5	717.5	28.7	-
<i>p</i> -value		P<0.05	P<0.05	1.0	0.1	P<0.05

Table 12 - The statistical analysis results on y-axis of all the computation assumptions in each state (with and without SnS) for subject B

		AUC [cm·sec]	Velocity [cm/sec]	Acceleration [cm/sec ²]	StS dura- tion [sec]	ANOVA Between signals
Without SnS	Average	617.0	-10.8	-0.1	3.1	-
	STD	12.0	0.4	0.2	0.1	-
With SnS	Average	194.3	-6.6	-0.5	2.5	-
	STD	24.3	0.9	0.9	0.3	-
Difference		68.5	38.7	68.5	17.4	-
<i>p</i> -value		P<0.05	0.3	1.0	0.1	P<0.05

Table 13 - The statistical analysis results on y-axis of all the computation assumptions in each state (with and without SnS) for subject C

		AUC [cm·sec]	Velocity [cm/sec]	Acceleration [cm/sec ²]	StS duration [sec]	ANOVA Between signals
Without SnS	Average	854.7	-6.4	0.1	4	-
	STD	37.0	1.0	0.3	0.2	-
With SnS	Average	429.6	-4.4	0.1	4.0	-
	STD	42.4	0.3	0.3	0.4	-
Difference		49.7	31.8	1.6	0.0	-
<i>p</i> -value		P<0.05	0.1	1.0	0.8	P<0.05

When comparing the results obtained from the statistical calculations for the three different subjects examined for the experiment, it can be recognized that, as received for x-axis also here, the p-value of the ANOVA between the signals were all under 0.05 for all of the examinees. In contrast to what seen for x-axis, here also the p-values for the AUC calculation was under 0.05 for all of the examinees as well. which means that there was a significant difference between the signals as well as between the AUC of StS with and without the SnS on y-axis. Besides, here, all of the relative differences were positive for all of the computational assumptions measured in this project, indicating the superiority of the SnS to gain stability.

6 Discussion

The system based on the LiDAR sensor embedded in the smartphone (iPhone Pro) was found to be suitable as a motion capture system and met the pre-defined requirements; portable, cheap, and easy to operate and one that requires simple data processing. This can be said due to combination of reasons. First, the system found to be consistent, so that for most of the measurements collected from the subjects examined by the system, the various repetitions (separated for state and axis) maintain a similar trend. Similar trends were also obtained between the different subjects (especially without the use of SnS device, divided into axes), and complementary opposite trends were seen between sitting and standing (appendix 9.2). Moreover, the general trends obtained correspond with the current findings, which are that the model obtained from the characterization of y-axis movement is equal to the model of StS movement as a function of GRF over time (Figure 2). Also, as it appears from the graphs, there is a relation between the axes results and there seem to be alignment between the axes, as the action that appear on one axis in a certain way occur at the same time on the other axis in a different manner. In addition, it has been proven that the system was sensitive to changes in the subject's movement (different initial position, different degree of bending, etc.).

Based on the data collected by the system and the data analysis performed on it, a movement graph of StS was obtained that corresponds with a known movement graph. As it appears (Figure 22 and appendix 9.2), the movement in x-axis includes the following characteristics; First, straight line (1) representing observed sitting. Afterwards, at the

beginning of the seat-off, a light upward peak called "positive peak" (2) can be recognized. The cause for this peak might be due to a brief leaning backward that supposed to provide some momentum to the standing action or due to slight bending forward so that the LiDAR measured the distance from the wall diagonally. The height of the peak depends on the degree of leaning backwards or bending forward respectively, as described. Afterward, a significant negative slope (3) ending in dominant downward peak called "negative peak" (4) is recognized which indicates the reduction of the measured distance. In light of the space where the experiment was performed, the greater the bending, the smaller distance measured by the system for the x-axis from the CoM to the floor therefore the slope of the graph is downwards. Meaning, that the dominant downward peak defines the extensiveness of the bending over during the standing action. Then, the graph's slope is going upwards (5), so the distance of the CoM from the floor increases. This increase in distance indicates the straightening of the subjects' back after the bending recorded beforehand. Next, another light positive peak (6) is recognized and right afterwards a steady line appears (7). The reason for this slight positive peak is probably due to the straitening of the back which changed the direction of the LiDAR's beam from the floor to the wall in front, so that the highest point of the peak should be the cross point of the wall to the floor, whereas the final state is a straight line which indicates a standing state. A few notes on this behalf should be noted; first, as it appears, the light positive peak at the beginning of the movement (2) is higher than the positive peak at the end of the recording (6). That probably since the pelvic of the subjects during the action changed its position so it went forward during the movement. For the same reason the steady-constant line at the beginning (1) that indicates the sitting posture is higher than the steady line at the end of the movement (7) which indicates the standing position, and as expected, during the StS movement the CoM is going forward.

As it appears (Figure 23 and appendix 9.2), the movement in y-axis includes the following properties; First, straight line (1) representing observed sitting. Then, a light negative peak can be recognized at the beginning of the movement (2). This slight peak is probably due to the start of the sit-off as the subject start to rise from the chair and thus results in a closer distance to the ceiling. However, right afterwards there is positive slope (3) that ends in a positive peak (4) which might indicate the bending over action, as the torso of the subject is directing diagonally towards the floor and thus the LiDAR beam at

the back directs in a diagonal angle to the ceiling so the distance which being measured is higher. The height of the peak is depending on the degree of the torso's bending forwards movement which results in greater angle between the LiDAR's beam and the ceiling and thus a higher distance was recorded. Then, a dominant slope downwards (5) appears which indicates both the rise of the subject upwards so the distance from the ceiling is getting lower during the standing action as well as the straitening of the torso so that the angle between the LiDAR's beam and the ceiling is getting closer to vertical (90 degrees) and thus the distance measured is shorter. Next, another light negative peak appears (6) right before the steady line (7). This negative peak might be due to the stabilization action up to a stable standing.

Additionally, when comparing the dominant negative peak on the x-axis to the dominant positive peak on y-axis it appears that the time when they occurred is similar. This supports the assumption that the subjects were performing bending forward, towards the floor, movement so that the LiDAR's beam on y-axis directed diagonally to the ceiling and as a result the distance from the CoM to the ceiling was higher.

The qualitative analysis was based on comparison between the graphs of the movement (position) over time with and without SnS device in both x and y axes to the video clips that recorded during the experiment per subject (appendix 9.1). This analysis was also compared to the average models obtained with and without using SnS (Figure 27), and accordingly, the following properties appear; first, the graphs show that the general nature of the movement is maintained with and without using SnS device, so it can be concluded that the StS movement characteristics are preserved during the use of SnS device, although there are some distinctions. The first difference was observed for the sitting state. In most of the graphs collected for y-axis, the steady state in the beginning of the recording was at a lower position than without the StS. This is due to the elevation of the subject's CoM higher in the chair by the SnS device's inflation with air and hence the distance measured between the CoM and the ceiling was shorter. The cases where the graphs don't seem lower with the SnS, is probably because of a tilt that made the direction of the LiDAR's beam hit diagonally on the ceiling and thus measuring longer distance. This explanation can be supported by Figure 25 and Figure 26. For example, when looking on subject 1 Appendix 9.1.1 which all its y-axis graphs without the SnS was lower than those with the SnS, when looking at the images with and without the SnS when the

subject sits, it can be recognized that she is leaning back while sitting on the SnS, probably in order to gain balance on the SnS device as the pillow pushes her CoM forward (as also demonstrated by the weight calculations in regard to Figure 21). This difference also affects the next step in y-axis, which is the negative peak obtained immediately after the session, which is usually lower with the use of SnS device. Moreover, the most significant change could be identified in the seat off phase in the slope and the peak obtained at the end (negative on the x-axis and positive on the y-axis), when most of the time the absolute values of the peaks were smaller with SnS device. One explanation for that is that the using of SnS device reduce the need for significant bending, considering bringing the CoM to a better starting point. Another explanation is that the starting point has an effect on the last two changes mentioned (i.e. the preparation for the seat off and the seat off). For example, when looking at the graphs and images of subject 4 (Appendix 9.1.4), the Subject started on the same position on the chair with and without the SnS, although while sitting on the SnS, the Subject bends his torso (which results in a higher position value at the starting position for both x and y axes with the SnS). It can be assumed that influenced by the sitting position on the SnS, the Subject had to bend his torso to gain stability while sitting. Additionally, when looking at his (subject 4) graphs on y-axis (Appendix 9.1.4), there is a more dramatic seat-off with the SnS, probably due to more extreme action of torso straitening. Therewith, it can be suggested that the preparation to seat-off influenced by the starting point posture. Further, the preparation to seat-off influenced by the subject's height as demonstrated by subject 2 (Appendix 9.1.2), who was relatively short and thus her location on the chair with the SnS demanded her to change the location of the CoM on the chair to be able to put her legs on the floor. Hence, the seat-off movement recorded in y axis for that Subject (4), was distinguishably different from the movement with the SnS in compare to the seat-off without it. Furthermore, for some of the subjects, different end points were observed (between repetitions of the same situations and between different situations) which resulted as such from the form of back alignment. Although, it is not possible to indicate a relationship between the degree of back alignment and the use of SnS device.

In general, it seems like the seat-off and vertical peak are most affected from the using of the SnS device.

Further, when comparing the graphs with and without in y-axis to those in x-axis, it appears, visually, that it's easier to distinguish between the graphs with or without using SnS device on y-axis in compared to x-axis. This finding has been supported by the results of the statistical measurements as well, which discuss next.

Regarding the effect of the SnS device, no unequivocal statements can be made based on the qualitative and quantitative analyzes performed. Although, some promising and important statements can be made. The quantitative analysis relied on 3 types of computational assumptions applied on the x-axis and y-axis (a total of 6 computational assumptions): AUC, velocity, and acceleration. The expectation was that increasing stability by using SnS device would be expressed through decreasing the values in the general equation on both axes. This expectation did not materialize for all computational assumptions. The computational measurement that was based on the calculation of the area under the curve (AUC) of the StS signals has a potential to appropriately distinguish between StS movements with and without SnS device's assistance as they found to have 25% success rate in both x and y axes, whereas the two other computational assumptions received 0% success rates. On the other hand, the comparison between the signals before applying the computational assumptions have found to provide the highest success rate in distinguishing between StS that has been performed with the use on SnS between a StS that has been performed without it, with 50% success rate. Following these outcomes, it can be concluded that there is a promising effect of the SnS on the StS movement, so that the structure of the StS motion is significantly being changed.

Moreover, under the assumption that the SnS device does improve the stability while performing StS Movement, the Acceleration assumptions has been found to best indicate the superiority of the use of the SnS device in both axes with 75% success rate in x-axis and 85.5% in y-axis and by that define stable and unstable of StS Movement. For the computational assumptions of velocity and AUC, no clear directionality was seen in the differences. This result indicates that although the Acceleration measurement could not significantly distinguish between the two maneuvers, it could indicate for superiority for the SnS to gain better stability by performing StS. Following that, it can be understand that a few improvements can be made to improve the experimental protocol in order to get more consist results.

From the results of the 2nd experimental trial, it can be concluded that y-axis better distinguishing between the StS with and without the SnS as well as providing a better indication for the superiority of the SnS device by gaining stability in the action. And yet, the 2nd trial was performed by only 3 subjects and thus not serve a reliable basis for statistical analysis.

Moreover, from the comparison of the duration of time it takes to perform StS with and without the use of SnS, as showed in Table 7, it was found that the use of SnS decrease the duration of time of the movement for all of the subjects participated, which implies that the use of SnS make it easier for the users to perform StS by shortening the activity's duration and thus the efforts that are being made for the StS action.

Besides that, the results obtained from the weight measurements reveals that the CoM's location transfers towards the BoS while sitting on the SnS device, with an average difference of 8.36 Kg in the 1st experimental session and 12.08 Kg in the 2nd. This finding strengthens the effectiveness of the SnS device in facilitating the StS motion by optimizing the user's stability. The stable standing position is achieved when the CoM aligns with the BoS. Therefore, as the CoM gradually shifts towards the BoS while in a seated position, the person is closer to standing. Consequently, the user experiences enhanced ease in transitioning from sitting to standing, requiring reduced effort to perform the StS action and providing valuable assistance.

For future experiments, a few recommendations and improvement suggestions can arise; first, the experiment should be conducted on a bigger group of Subjects for more statistically support and to reduce the error rate and the influence of exceptions on the analysis and conclusions. Also, it is important to test subjects that are more relevant to the experiment, i.e., subjects with mobility issues and difficulty in performing StS. In addition, the experiment conditions should be improved, as discussed and implemented for the improved experimental trail, marking the position of sitting on the chair so it will be similar to the position on the SnS, as well as marking the position of the legs on the floor while standing (and measure the difference in position in case their location have changes during the movement). Also, ensure back straightening during the experiment as much as possible. Besides, it can be suggested to examine only one axis, and especially y axis which found as better distinguishing between the movement of SnS with and with-

out SnS and also obtained higher success rated for the statistical measurements as previously discussed. As it discovered through the analysis, the information obtained from the y-axis alone is adequate for investigation of the StS movement. Further, in case the two axes are being measured, in order to prevent the direction of the LiDAR towards the floor while leaning over during the movement, it is possible to create iPhone mount which equipped with a corner hinge which prevent the tilting of the iPhone during the leaning over so that the LiDAR remains oriented toward the wall at a 90-degree angle along the entire measurement.

7 Conclusion

The project described in this report had three main goals to implement; first, create a new method to trace Sit-to-Stand movement, which will be low-cost, mobile and easy to analyze as well as evaluate the ability of this method to successfully trace the StS maneuver. Second, produce computational model's assumptions to assess stability and instability of StS Movement. And the last goal was to evaluate the SnS device's success to improve stability during StS Movement.

Due to these goals, in this project, a new method was planned and implemented using two iPhone Pro smartphones with built-in LiDAR sensors and wearable belts system which designed to hold the smartphones in a stable and adjustable manner. The LiDAR sensors were placed adjacent to the subject's center of mass (CoM) and measured the distance of CoM from permanent surfaces to measure the StS Movement in two axes. Additionally, three computational method's assumptions were written, considering the characteristics of stability and instability StS Movement as described in the literature. The necessity for this computational assumption was since the method established in this project was never used before and thus equivalent results were never assessed beforehand. Then, the computational assumptions were calculated over a data collected from 8 old examined conducted StS with and without the assistance of SnS device wearing the belt system designed to hold the two iPhone Pro smartphones.

The main goal of the project, which was to create a new method of motion capturing system based on the LiDAR sensor in smart phones (iPhones from the Pro series) achieved. The system developed in the project and tested found to meet the requirements and resulted in a quality movement description of StS.

Alongside this, it is not possible to decide on the relevance of all the computational assumptions due to the low success rates obtained from the ANOVA test suggesting that there was no highly significant difference between the results of the computational assumptions.

while considering the limitations that described, out of the computational assumptions that have been evaluated during this project, AUC is the measurement which most significantly distinguish between StS with and without SnS with the highest success rate of 25% for both x and y axes. On the other hand, there was 50% success rate for both axes from the comparison conducted between the positions of the CoM during the movement. Besides, the relative difference results had higher success rates with 75% and 85.5% for x and y axis respectively, negative relative difference for the Acceleration assumptions which indicates superiority for the use of SnS for the assumption and by that suggests that the use of SnS can contribute to the stability of the users when performing StS, especially when measured on signals provided from y-axis (when LiDAR's beam was directing to the ceiling).

Additionally, The SnS found to decrease the extent of leaning over action during StS in both axes, and hence improves the stability of the users while performing StS.

Over and above, through weight measurements, it has been observed that the SnS significantly influences the CoM position when seated. As a result, it can be inferred that utilizing the SnS aids the user in executing the StS movement more effortlessly. The SnS provides an advantageous starting point for the transition from sitting to standing, as the CoM position is already considerably closer to the BoS while seated on the SnS.

Meanwhile, the experiment was not ideal as not all the participants had mobility difficulties or any struggle conducting StS, and the number of participants in the experiment is not sufficient for statistical analysis. So, a follow-up experiment with a larger number of relevant subjects should be conducted. Also, if the computational assumption relied on is AUC, it is recommended to examine in the next experiment the possibility of reducing the system to one phone on the y-axis. Further, in order to eliminate the effect of the LiDAR directing to the floor, a new mount can be used which allows tilting of the iPhone so that the LiDAR beam will direct vertically to the wall in front along the entire measurement. Additionally, it is possible that ensuring straitening of the back during the StS movement can improve the accuracy of the results, as well as marking the location of the

sitting on the chair so it will match the location of sitting on the SnS device when its fully inflated.

8 References

- [1] Bahrami, F., Riener, R., Jabedar-Maralani, P., & Schmidt, G. (2000). Biomechanical analysis of sit-to-stand transfer in healthy and paraplegic subjects. In Clinical Biomechanics (Vol. 15, Issue 2, pp. 123–133). Elsevier BV. [https://doi.org/10.1016/s0268-0033\(99\)00044-3](https://doi.org/10.1016/s0268-0033(99)00044-3)
- [2] Fletcher, L., Cornall, C., & Armstrong, S. (2009). Moving between sitting and standing. *Bobath Concept*, 83-116.
- [3] Zhou, B., Xue, Q., Yang, S., Zhang, H., & Wang, T. (2021). Design and control of a sit-to-stand assistive device based on analysis of kinematics and dynamics. In Automatika (Vol. 62, Issues 3–4, pp. 353–364). Informa UK Limited. <https://doi.org/10.1080/00051144.2021.1967603>
- [4] van der Kruk, E., Strutton, P., Koizia, L.J. et al. Why do older adults stand-up differently to young adults?: investigation of compensatory movement strategies in sit-to-walk. *npj Aging* 8, 13 (2022). <https://doi.org/10.1038/s41514-022-00094-x>
- [5] Galli, M., Cimolin, V., Crivellini, M., & Campanini, I. (2008). Quantitative analysis of sit to stand movement: Experimental set-up definition and application to healthy and hemiplegic adults. In *Gait & Posture* (Vol. 28, Issue 1, pp. 80–85). Elsevier BV. <https://doi.org/10.1016/j.gaitpost.2007.10.003>
- [6] Bennett, T., Kumar, P., & Garate, V. R. (2022). A Machine Learning Model for Predicting Sit-to-Stand Trajectories of People with and without Stroke: Towards Adaptive Robotic Assistance. In Sensors (Vol. 22, Issue 13, p. 4789). MDPI AG. <https://doi.org/10.3390/s22134789>
- [7] S. Mefoued, S. Mohammed, Y. Amirat and G. Fried, "Sit-to-Stand movement assistance using an actuated knee joint orthosis," 2012 4th IEEE RAS & EMBS International Conference on Biomedical Robotics and Biomechatronics (BioRob), 2012, pp. 1753-1758, doi: 10.1109/BioRob.2012.6290830.
- [8] Komisar, V., van Schooten, K. S., Aguiar, O. M. G., Shishov, N., & Robinovitch, S. N. (2022). Circumstances of Falls During Sit-to-Stand Transfers in Older People: A Cohort Study of Video-Captured Falls in Long-Term Care. In Archives of Physical Medicine and Rehabilitation. Elsevier BV. <https://doi.org/10.1016/j.apmr.2022.10.012>
- [9] Holmes, P. D., Danforth, S. M., Fu, X.-Y., Moore, T. Y., & Vasudevan, R. (2020). Characterizing the limits of human stability during motion: perturbative experiment validates a model-based approach for the Sit-to-Stand task. In Royal Society Open Science (Vol. 7, Issue 1, p. 191410). The Royal Society. <https://doi.org/10.1098/rsos.191410>
- [10] Fujimoto, M., & Chou, L.-S. (2013). Region of Stability Derived by Center of Mass Acceleration Better Identifies Individuals with Difficulty in Sit-to-Stand Movement. In Annals of Biomedical Engineering (Vol. 42, Issue 4, pp. 733–741). Springer Science and Business Media LLC. <https://doi.org/10.1007/s10439-013-0945-9>
- [11] Older Adult Falls—Costly But Not Inevitable, HEALTH AFFAIRS FOREFRONT, APRIL 4, 2018, 10.1377/forefront.20180402.25780, <https://www.healthaffairs.org/do/10.1377/forefront.20180402.25780/>
- [12] Older Adult Fall Prevention, centers for disease control and prevention, <https://www.cdc.gov/falls/index.html>
- [13] M. H. Nematollahi, S. A. Haghpanah and S. Taghvaei, "Inverse dynamic tracking control of sitting and standing movement," 2018 25th National and 3rd International Iranian Conference on Biomedical Engineering (ICBME), 2018, pp. 1-6, doi: 10.1109/ICBME.2018.8703584.
- [14] Rea, P., & Ottaviano, E. (2016). Analysis and mechanical design solutions for sit-to-stand assisting devices, *American Journal of Engineering and Applied Sciences*
- [15] R. P. Matthew, S. Seko, J. Bailey, R. Bajcsy and J. Lotz, "Estimating Sit-to-Stand Dynamics Using a Single Depth Camera," in IEEE Journal of Biomedical and Health Informatics, vol. 23, no. 6, pp. 2592-2602, Nov. 2019, doi: 10.1109/JBHI.2019.2897245.
- [16] P. O. Riley, M. L. Schenkman, R. W. Mann and W. A. Hodge, "Mechanics of a constrained chair-rise", *J. Biomechanics*, vol. 24, no. 1, pp. 77-85, 1991
- [17] Janssen, W. G., Bussmann, H. B., & Stam, H. J. (2002). Determinants of the Sit-to-Stand Movement: A Review. In *Physical Therapy* (Vol. 82, Issue 9, pp. 866–879). Oxford University Press (OUP). <https://doi.org/10.1093/ptj/82.9.866>
- [18] Aissaoui, R., & Dansereau, J. (n.d.). Biomechanical analysis and modelling of sit to stand task: a literature review. In IEEE SMC'99 Conference Proceedings. 1999 IEEE International Conference

- on Systems, Man, and Cybernetics (Cat. No.99CH37028). IEEE SMC'99 Conference Proceedings. 1999 IEEE International Conference on Systems, Man, and Cybernetics. IEEE. <https://doi.org/10.1109/icsmc.1999.814072>
- [19] Mao, Y. R., Wu, X. Q., Zhao, J. L., Lo, W. L. A., Chen, L., Ding, M. H., Xu, Z. Q., Bian, R. H., Huang, D. F., & Li, L. (2018). The Crucial Changes of Sit-to-Stand Phases in Subacute Stroke Survivors Identified by Movement Decomposition Analysis. In *Frontiers in Neurology* (Vol. 9). Frontiers Media SA. <https://doi.org/10.3389/fneur.2018.00185>
- [20] Chorin, F., Cornu, C., Beaune, B., Frère, J., & Rahmani, A. (2015). Sit to stand in elderly fallers vs non-fallers: new insights from force platform and electromyography data. In *Aging Clinical and Experimental Research* (Vol. 28, Issue 5, pp. 871–879). Springer Science and Business Media LLC. <https://doi.org/10.1007/s40520-015-0486-1>
- [21] Salah, O., Asker, A., Fath El-Bab, A. M. R., Assal, S. M. F., Ramadan, A. A., Sessa, S., & Abo-Ismail, A. (2013). Development of parallel manipulator sit to stand assistive device for elderly people. In 2013 IEEE Workshop on Advanced Robotics and its Social Impacts. 2013 IEEE Workshop on Advanced Robotics and its Social Impacts (ARSO). IEEE. <https://doi.org/10.1109/arso.2013.6705501>
- [22] Mourey, F., Pozzo, T., Rouhier-Marcer, I., & Didier, J. P. (1998). A kinematic comparison between elderly and young subjects standing up from and sitting down in a chair. *Age and ageing*, 27(2), 137-146. <https://elibrary.mediun.edu.my/books/2017/MEDIU05772.pdf>
- [23] Dubost, V., Beauchet, O., Manckoundia, P., Herrmann, F., & Mourey, F. (2005). Decreased Trunk Angular Displacement During Sitting Down: An Early Feature of Aging. In *Physical Therapy* (Vol. 85, Issue 5, pp. 404–412). Oxford University Press (OUP). <https://doi.org/10.1093/ptj/85.5.404>
- [24] Schultz, A. B., Alexander, N. B., & Ashton-Miller, J. A. (1992). Biomechanical analyses of rising from a chair. *Journal of Biomechanics*, 25(12). [https://doi.org/10.1016/0021-9290\(92\)90052-3](https://doi.org/10.1016/0021-9290(92)90052-3)
- [25] Fujimoto, M., & Chou, L. S. (2012). Dynamic balance control during sit-to-stand movement: An examination with the center of mass acceleration. *Journal of Biomechanics*, 45(3). <https://doi.org/10.1016/j.jbiomech.2011.11.037>
- [26] Chen, T., & Chou, L. S. (2013). Altered center of mass control during sit-to-walk in elderly adults with and without history of falling. *Gait and Posture*, 38(4). <https://doi.org/10.1016/j.gaitpost.2013.03.007>
- [27] Liang, S., Ning, Y., Li, H., Wang, L., Mei, Z., Ma, Y., & Zhao, G. (2015). Feature Selection and Predictors of Falls with Foot Force Sensors Using KNN-Based Algorithms. In *Sensors* (Vol. 15, Issue 11, pp. 29393–29407). MDPI AG. <https://doi.org/10.3390/s151129393>
- [28] Piano, L., Geri, T. & Testa, M. Raising and stabilization phase of the sit-to-stand movement better discriminate healthy elderly adults from young subjects: a pilot cross-sectional study. *Arch Physiother* 10, 7 (2020). <https://doi.org/10.1186/s40945-020-00078-8>
- [29] Mombaur, K., & Ho Hoang, K.-L. (2017). How to best support sit to stand transfers of geriatric patients: Motion optimization under external forces for the design of physical assistive devices. In *Journal of Biomechanics* (Vol. 58, pp. 131–138). Elsevier BV. <https://doi.org/10.1016/j.jbiomech.2017.04.037>
- [30] SitnStand, Portable Smart Rising Seats (SnS), <https://www.sitnstand.com/>
- [31] Brščić, D., Evans, R. W., Rehm, M., & Kanda, T. (2020). Using a Rotating 3D LiDAR on a Mobile Robot for Estimation of Person's Body Angle and Gender. In *Sensors* (Vol. 20, Issue 14, p. 3964). MDPI AG. <https://doi.org/10.3390/s20143964>
- [32] Aditya K B, Deepak S (2017). LIDAR TECHNOLOGY AND APPLICATIONS. EPRA International Journal of Research and Development (IJRD) (Vol. 2, Issue 3). https://eprajournals.com/jpanel/upload/1215am_27_Aditya%20Kumar%20Bhatt-1108.pdf
- [33] King, F., Kelly, R., & Fletcher, C. G. (2022). Evaluation of LiDAR-Derived Snow Depth Estimates From the iPhone 12 Pro. In *IEEE Geoscience and Remote Sensing Letters* (Vol. 19, pp. 1–5). Institute of Electrical and Electronics Engineers (IEEE). <https://doi.org/10.1109/lgrs.2022.3166665>
- [34] Luetzenburg, G., Kroon, A., & Bjørk, A. A. (2021). Evaluation of the Apple iPhone 12 Pro LiDAR for an Application in Geosciences. *Scientific Reports*, 11(1). <https://doi.org/10.1038/s41598-021-01763-9>
- [35] Instron 5544 – Tensile Tester, The Lab world group <https://www.thelabworldgroup.com/product/instron-5544-tensile-tester/>.

- [36] Atrsaei, A., Paraschiv-Ionescu, A., Krief, H., Henchoz, Y., Santos-Eggimann, B., Büla, C., & Aminian, K. (2021). Instrumented 5-Time Sit-To-Stand Test: Parameters Predicting Serious Falls beyond the Duration of the Test. In Gerontology (Vol. 68, Issue 5, pp. 587–600). S. Karger AG. <https://doi.org/10.1159/000518389>
- [37] www.vieyrasoftware.net ([link to App Store](#))
- [38] Arfken GB, Griffing DF, Kelly DC, Priest J, University Physics, Elsevier, 1984

9 Appendix

9.1 Appendix A – Per Subject Analysis

9.1.1 Subject 1

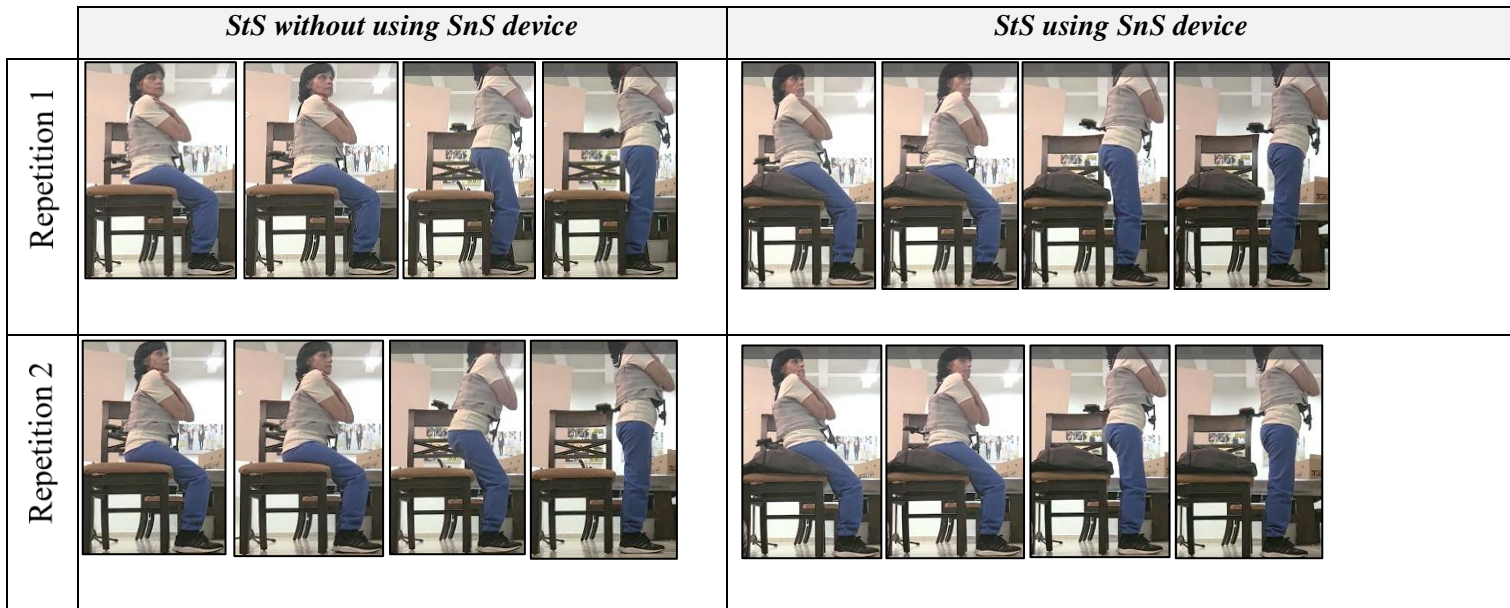
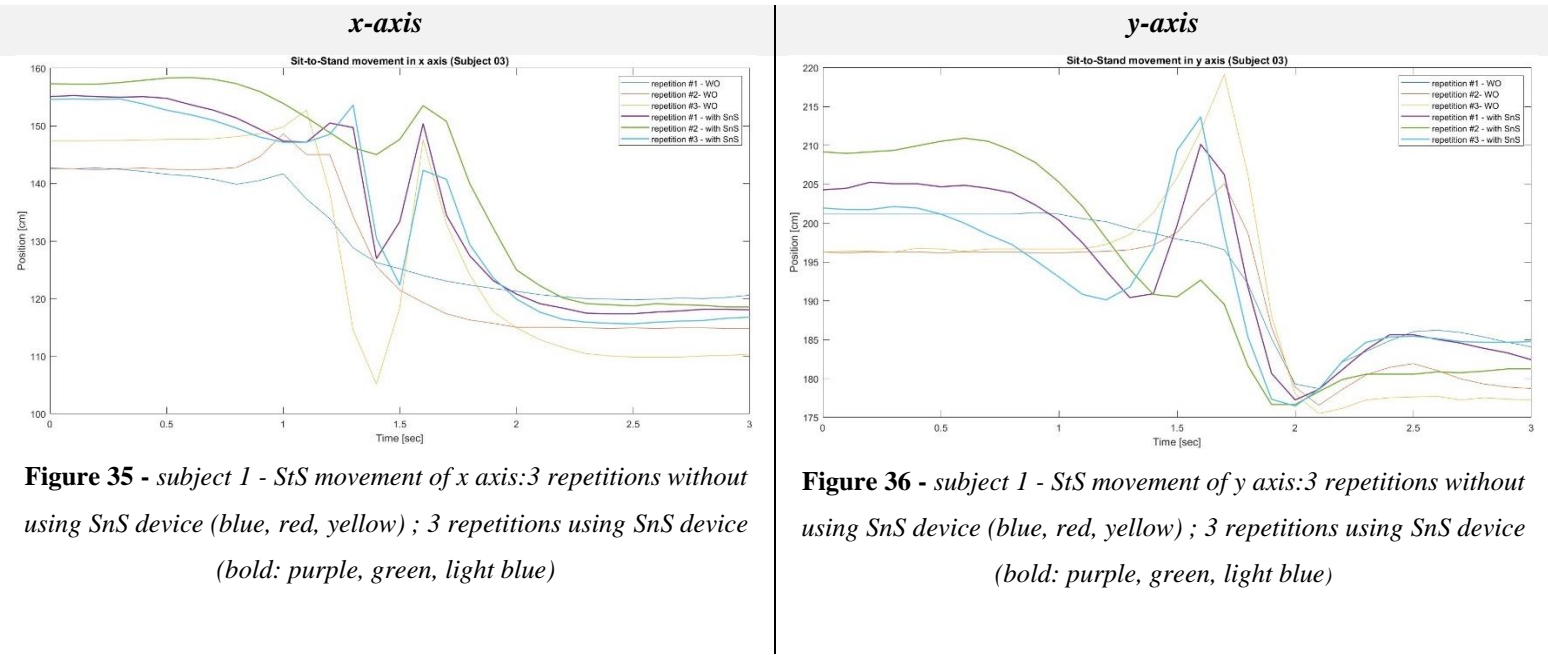


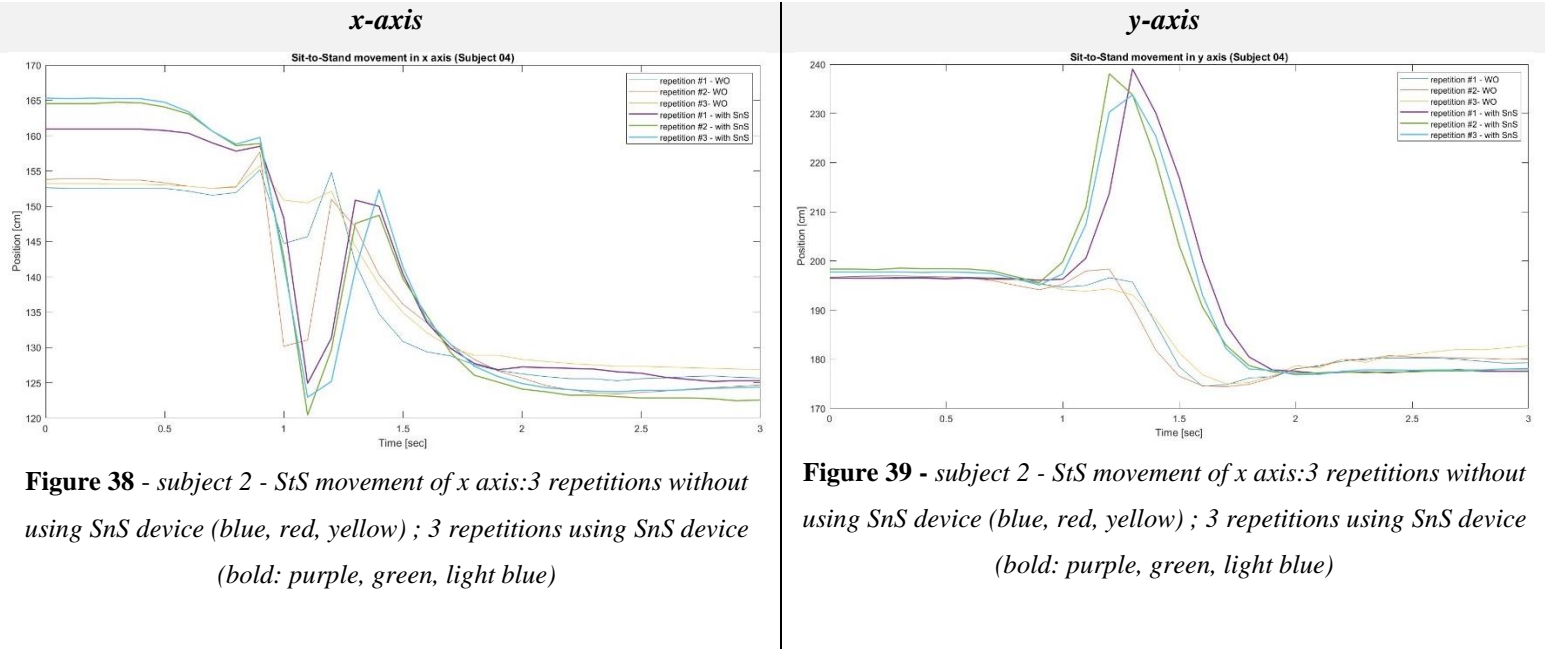


Figure 37 - subject 1 - Selected videos of StS movement with and without using SnS device

As can be seen in Fig.## and Fig.## above, there is an overall resembles in StS movement structure over time in both axes with and without the SnS device. Also, a relation between the axes can be recognized as differences occurred on graph in one axis during the movement at a certain time period, at the same time period a difference can be seen on the other axis. Additionally, the graph of y-axis resembles to the graph on Fig. 2 in the introduction.

When looking at the attached images on Fig.### it seems as the preparation to seat-off influenced by the starting point, so that the Subject need to straighten the torso before standing. Besides, with the use of the SnS, the distance of the CoM in both axes is longer, that is caused by the difference in the Subject's body posture when sitting with and without the SnS. In addition, there is a difference between the StS movement within the same state, for example, on the two first repeats without the SnS no bending forward conducted, whereas on the third repeat very dominant bending was performed. Especially in y-axis, this may have resulted in the lack of significance in the AUC value in this axis (Table 4).

9.1.2 Subject 2



Due to a technical fault, there is no video recording of subject 2. Therefore, the analysis was based on the graphs and the assumption calculations only.

As it appears from the graphs on Fig.## and Fig.## above, there is an overall resembles in StS movement structure over time in both axes with and without the SnS device. Also, a relation between the axes can be recognized as differences occurred on graph in one axis during the movement at a certain time period, at the same time period a difference can be seen on the other axis. Additionally, the graph of y-axis resembles to the graph on Fig. 2 in the introduction. Besides, from the graph of y-axis there is a clear difference between the peaks in the graphs occurred for the StS with the SnS compared to the peaks without the SnS which were all dramatically lower. The change is so significant that all the calculated results obtained on the Y axis were significant, in a positive direction. The end point is the same in all repetitions.

9.1.3 Subject 3

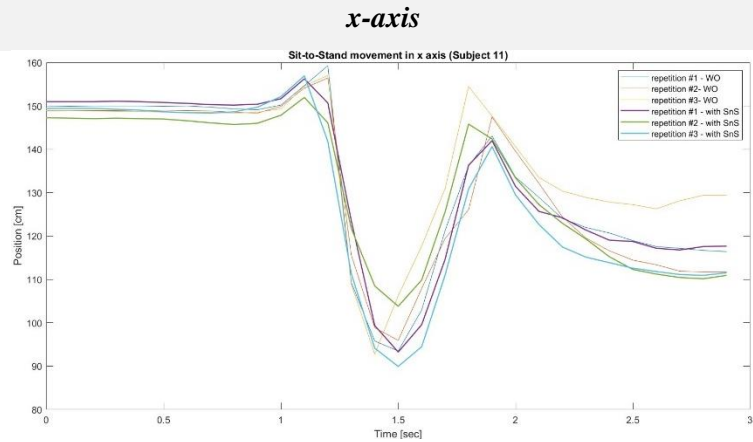


Figure 40 - subject 3 - StS movement of x axis:3 repetitions without using SnS device (blue, red, yellow) ; 3 repetitions using SnS device (bold: purple, green, light blue)

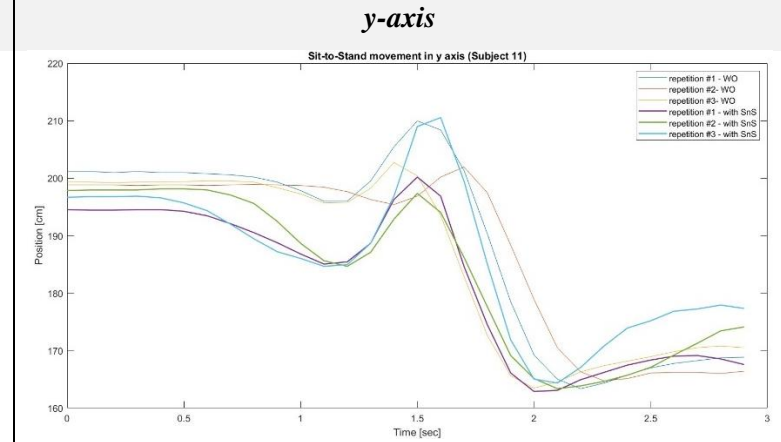


Figure 41 - subject 3 - StS movement of x axis:3 repetitions without using SnS device (blue, red, yellow) ; 3 repetitions using SnS device (bold: purple, green, light blue)

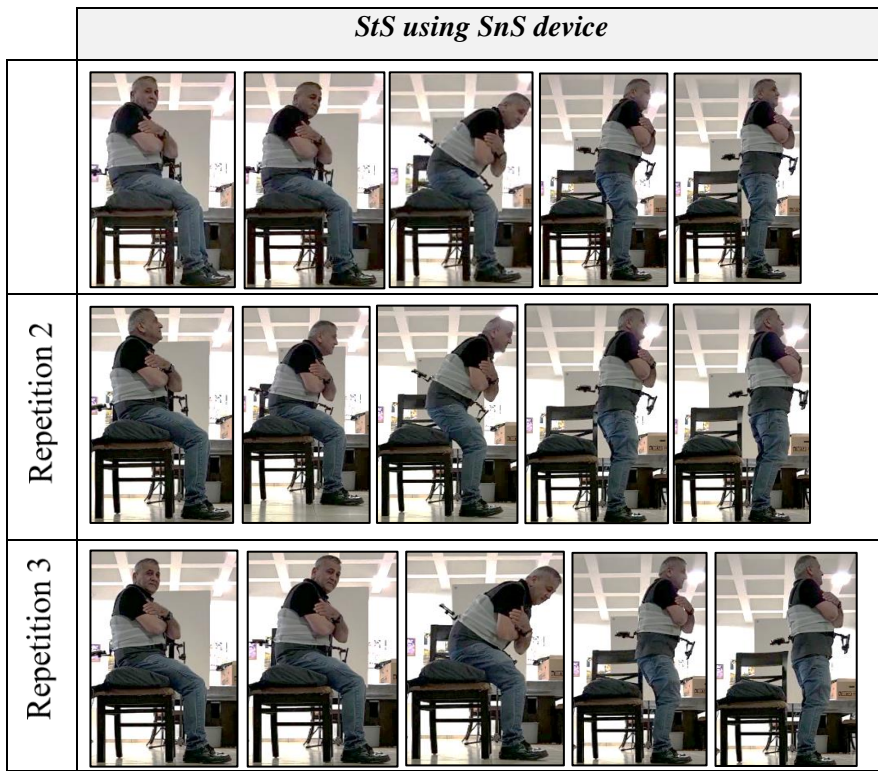


Figure 42 - subject 3 - Selected videos of StS movement using SnS device

Due to a technical fault, there is no video recording of subject 3 without using SnS device. From the graphs on Fig.## and Fig.## above, there is an overall resemblance in

StS movement structure over time in both axes with and without the SnS device. Also, a relation between the axes can be recognized as differences occurred on graph in one axis during the movement at a certain time period, at the same time period a difference can be seen on the other axis. Additionally, the graph of y-axis resembles to the graph on Fig. 2 in the introduction. The starting point (sitting) on x-axis is further away without using SnS device, probably because the subject sat further in in the chair without SnS device. The distance on y-axis is lower due to the inflation of SnS device. Also, the preparation for seat off is more significant in y-axis using SnS device. The seat off phase is different in repetitions of the same situation. When looking at the attached images on Fig.### it seems as there was a difference between the StS movement within the same state, for example, the degree of torso bending in the third repeat seems much higher than the bending performed on the other repeats and in relation to that occurrence, the graph for the third repeat with the SnS has a higher peak than the others. The final stage of standing is different, so considering the degree of straightening of the back.

9.1.4 Subject 4

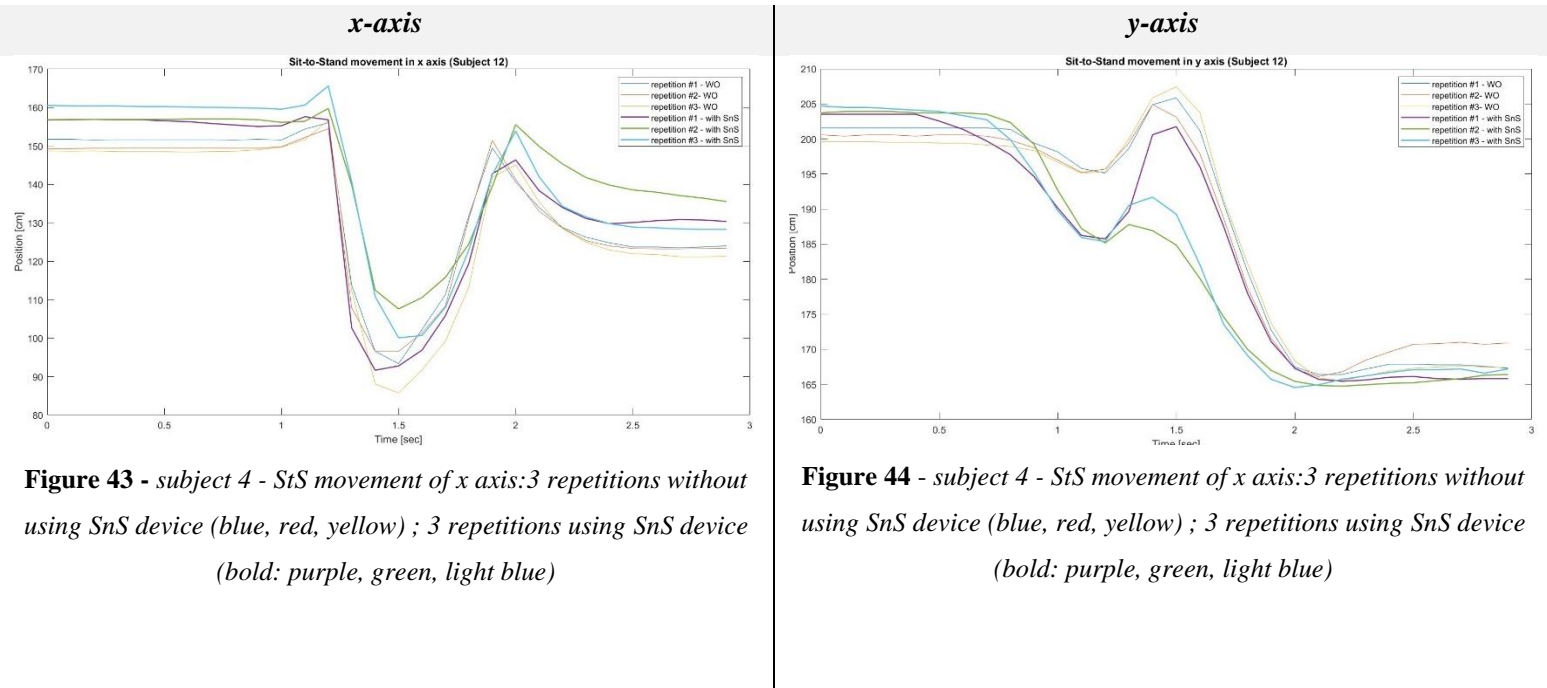


Figure 43 - subject 4 - StS movement of x axis:3 repetitions without using SnS device (blue, red, yellow) ; 3 repetitions using SnS device (bold: purple, green, light blue)

Figure 44 - subject 4 - StS movement of x axis:3 repetitions without using SnS device (blue, red, yellow) ; 3 repetitions using SnS device (bold: purple, green, light blue)

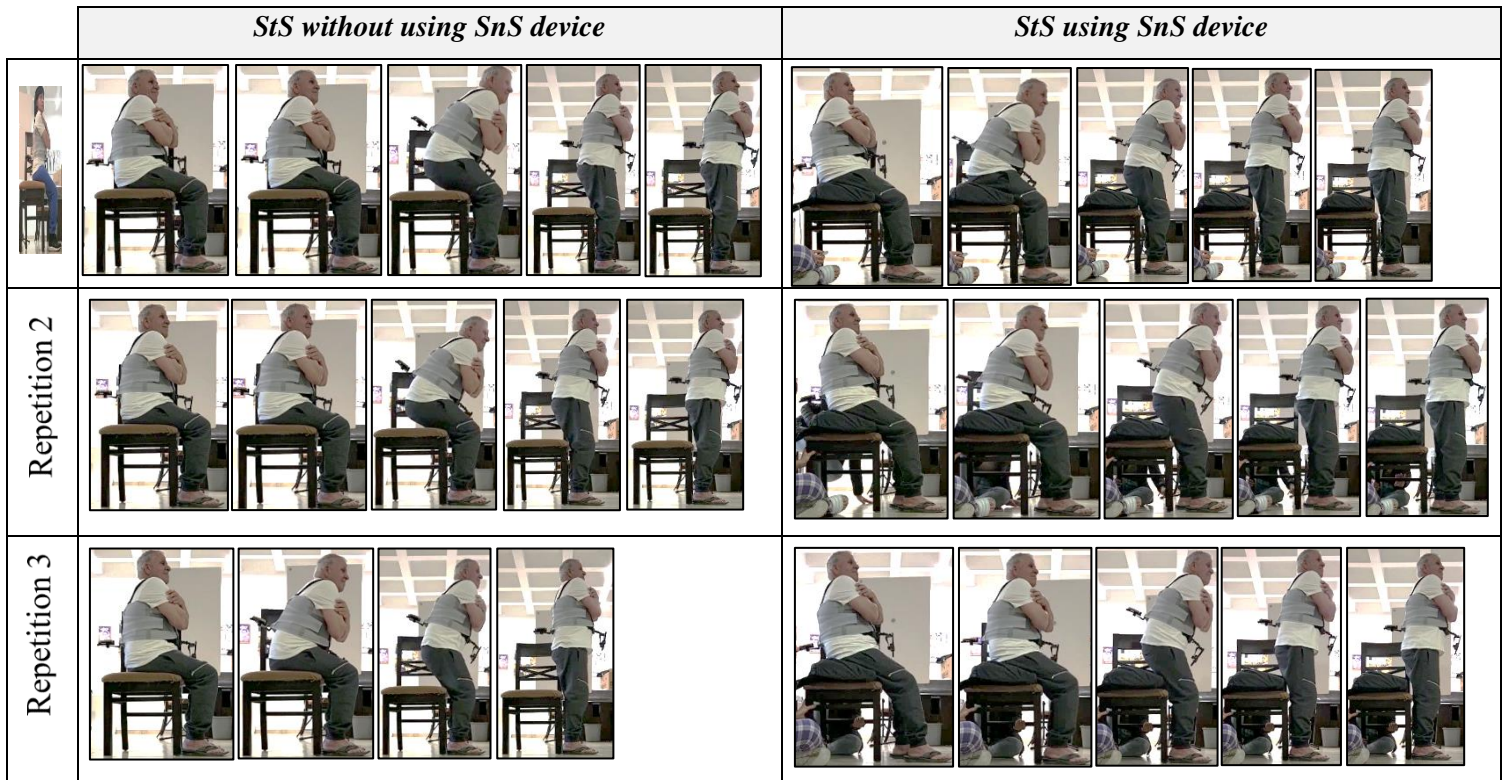


Figure 45 - subject 4 - Selected videos of StS movement with and without using SnS device

From the graphs on Fig.## and Fig.## above, there is an overall resembles in StS movement structure over time in both axes with and without the SnS device. Also, a relation between the axes can be recognized as differences occurred on graph in one axis during the movement at a certain time period, at the same time period a difference can be seen on the other axis. Additionally, the graph of y-axis resembles to the graph on Fig. 2 in the introduction. When looking at the attached images on Fig.### it seems as there was a difference between the StS movement. Significance is reflected in both axes for the computational assumption AUC. First, the starting point is different when in both axes the distance is greater when using SNS device that resulted from sitting with the back leaning back. This is how it affected the preparation for the seat off as well as the degree of bending - there is a difference in the seat-off with and without the SnS as clearly seen on the y-axis. Additionally, from the images attached on Fig.## it appears that there was less bending action while using the SnS device. It can also be seen that there was a match between the degree of bending - for example in the first repetition using SnS Device both in the pictures and in the graph that there was a more significant bending. Here too, the final stage of standing is different, so considering the degree of straightening of the back.

9.1.5 Subject 5

x-axis

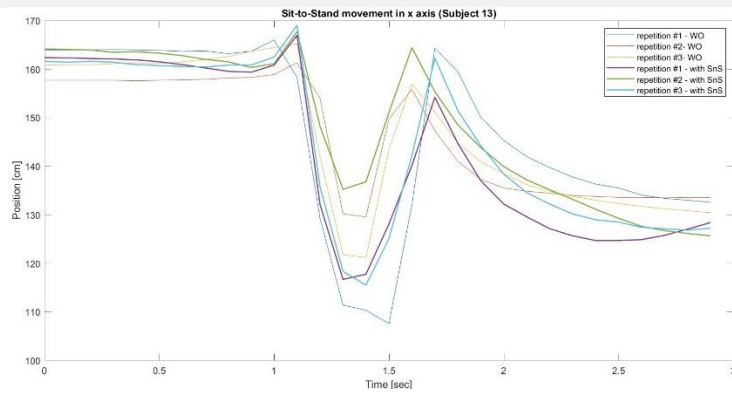


Figure 46 - subject 5 - StS movement of x axis:3 repetitions without using SnS device (blue, red, yellow) ; 3 repetitions using SnS device (bold: purple, green, light blue)

y-axis

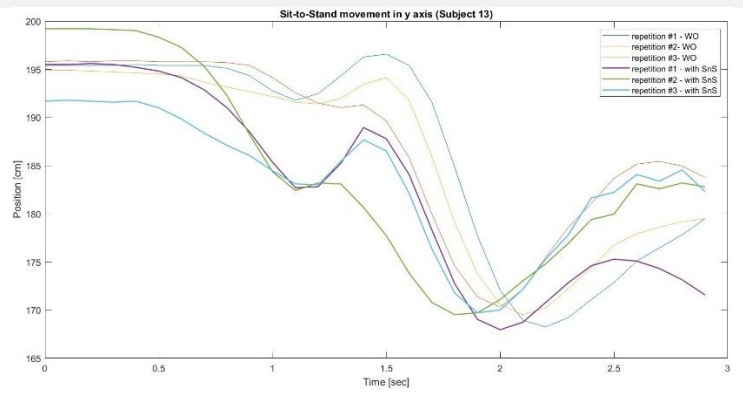


Figure 47 - subject 5 - StS movement of x axis:3 repetitions without using SnS device (blue, red, yellow) ; 3 repetitions using SnS device (bold: purple, green, light blue)

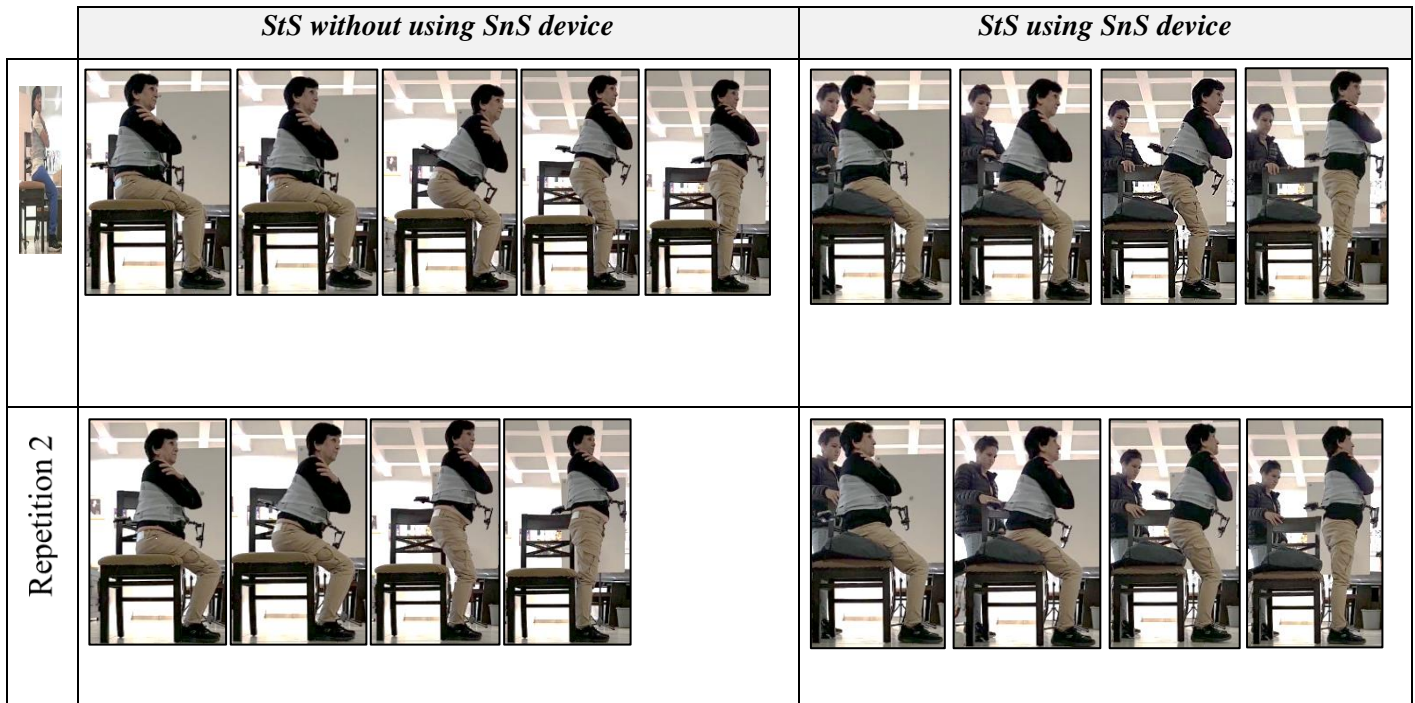




Figure 48 - subject 5 - Selected videos of StS movement with and without using SnS device

As it seems from the graphs on Fig.## and Fig.## above, there is an overall resemblance in StS movement structure over time in both axes with and without the SnS device. Also, a relation between the axes can be recognized as differences occurred on graph in one axis during the movement at a certain time period, at the same time period a difference can be seen on the other axis. Additionally, the graph of y-axis resembles to the graph on Fig. 2 in the introduction. On the other hand, the graphs on y-axis distinguish from each other for the three repeats conducted with the SnS device. As it visually recognized, the green graph, of the second repeat starts with the highest position, then after around 1.5 seconds it has the lowest position, and it ends in the middle. In the same manner, the other graphs seem to change their relation to the others along the movement. When looking at the attached images on Fig.### it seems as there was a difference in the degree of torso bending during the StS movement. Also, in the second repeat the degree of bending seems lowest between the other bending actions recorded with the SnS, whereas the starting position for that repeat seem also different with a leaning backwards in the beginning of the movement.

9.1.6 Subject 6

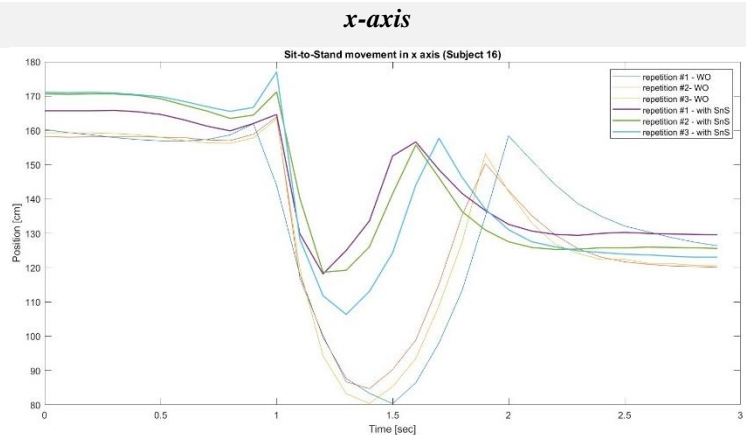


Figure 49 - subject 6 - StS movement of x axis:3 repetitions without using SnS device (blue, red, yellow) ; 3 repetitions using SnS device (bold: purple, green, light blue)

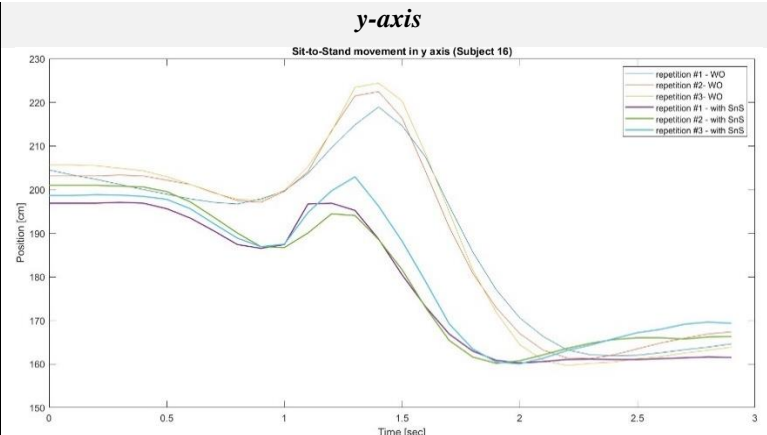


Figure 50 - subject 6 - StS movement of x axis:3 repetitions without using SnS device (blue, red, yellow) ; 3 repetitions using SnS device (bold: purple, green, light blue)

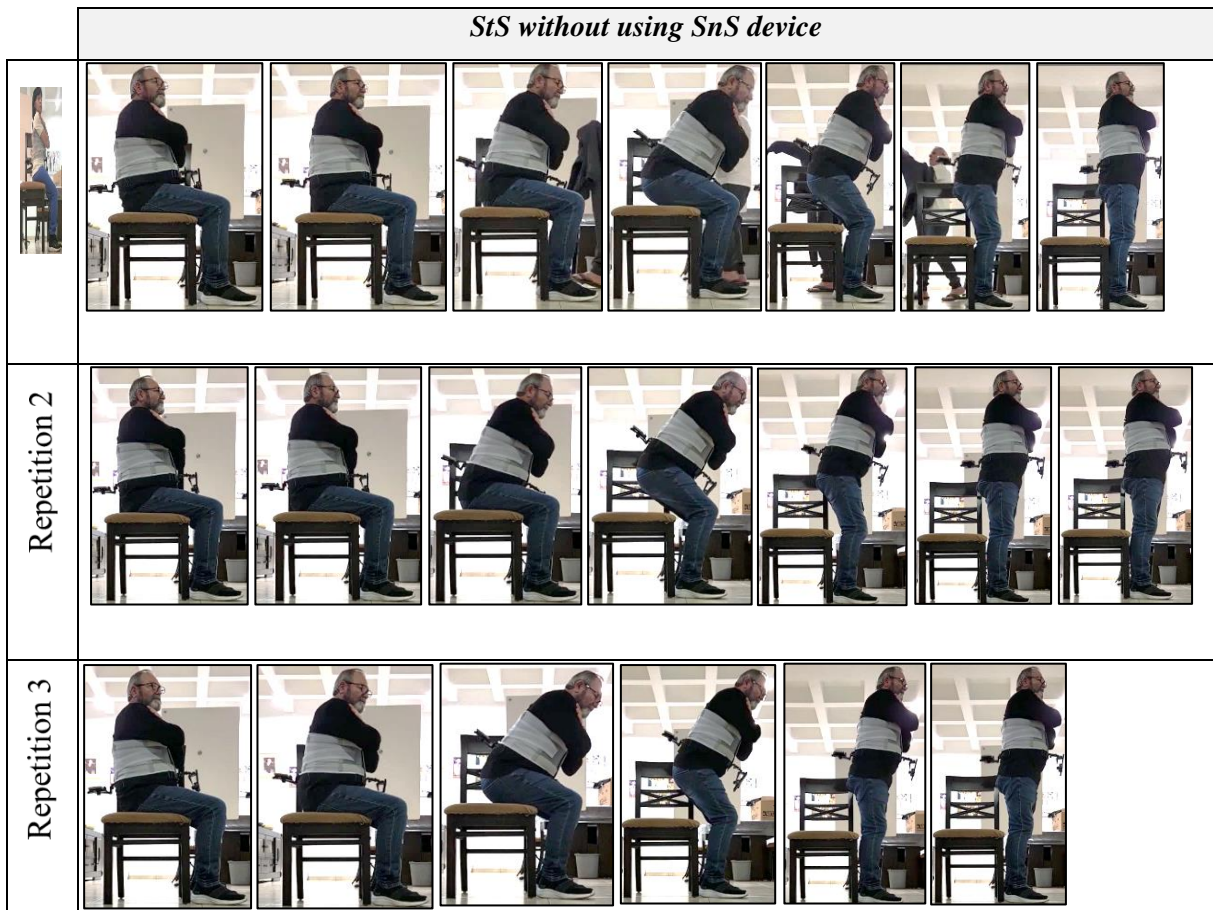


Figure 51 - subject 6 - Selected videos of StS movement without using SnS device

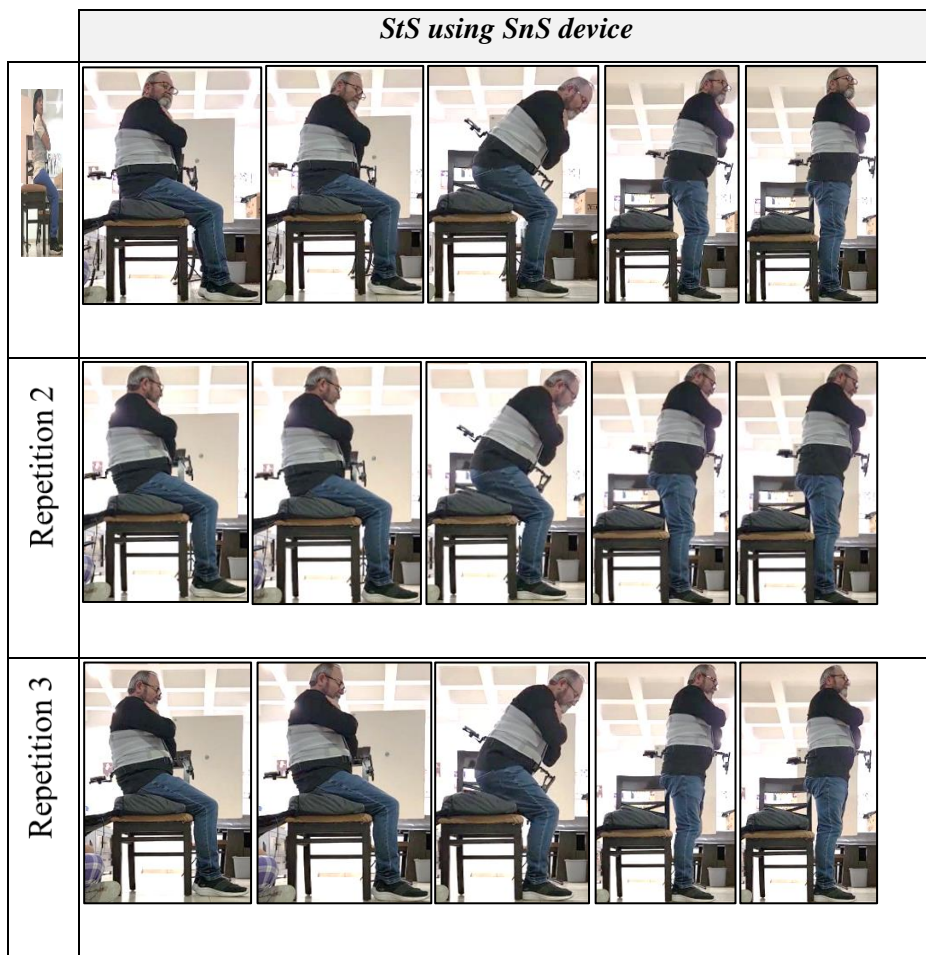


Figure 52 - subject 6 - Selected videos of StS movement using SnS device

As appear from the graphs on Fig.## and Fig.## above, there is an overall resembles in StS movement structure over time in both axes with and without the SnS device. Also, a relation between the axes can be recognized as differences occurred on graph in one axis during the movement at a certain time period, at the same time period a difference can be seen on the other axis. Additionally, the graph of y-axis resembles to the graph on Fig. 2 in the introduction. On the other hand, the graphs on both axes distinguish from each other for the three repeats conducted with the SnS device in compared to those without it. The differences were seen in two main trends: smaller peaks (in absolute value) with an SNS device, and a shorter time to perform the movement. Meaning, it seems like the seat-off is most affected by whether there was or wasn't use of SnS device for the StS. When looking at the attached images on Fig.### it seems as there were differences in the

starting body posture with and without the SnS. From the images it appears that without the SnS the subject sat with his back straight whereas when he sat on the SnS his back bend backwards (in the last two repetitions using SnS device).

For this subject significant result were seen (Table 4) for AUC and velocity in both axes.

9.1.7 Subject 7

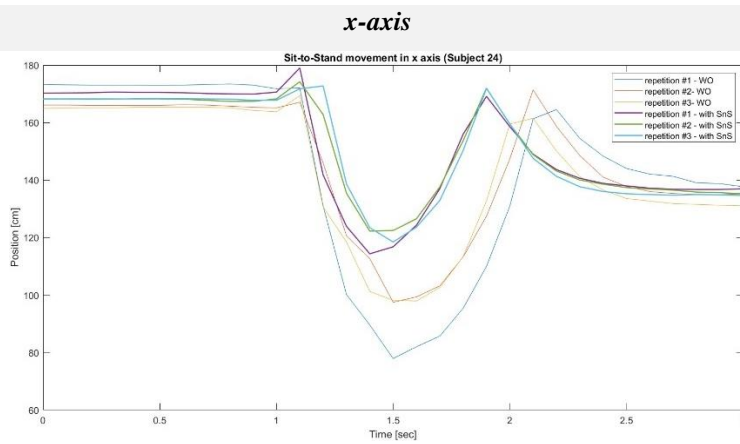


Figure 53 - subject 7 - StS movement of x axis:3 repetitions without using SnS device (blue, red, yellow) ; 3 repetitions using SnS device (bold: purple, green, light blue)

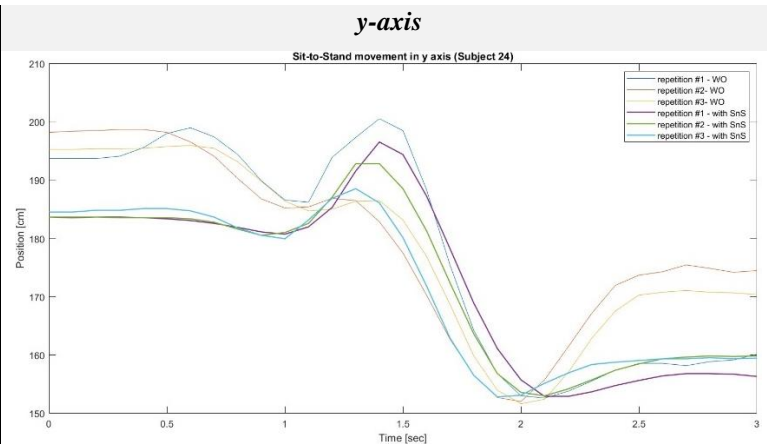


Figure 54 - subject 7 - StS movement of x axis:3 repetitions without using SnS device (blue, red, yellow) ; 3 repetitions using SnS device (bold: purple, green, light blue)

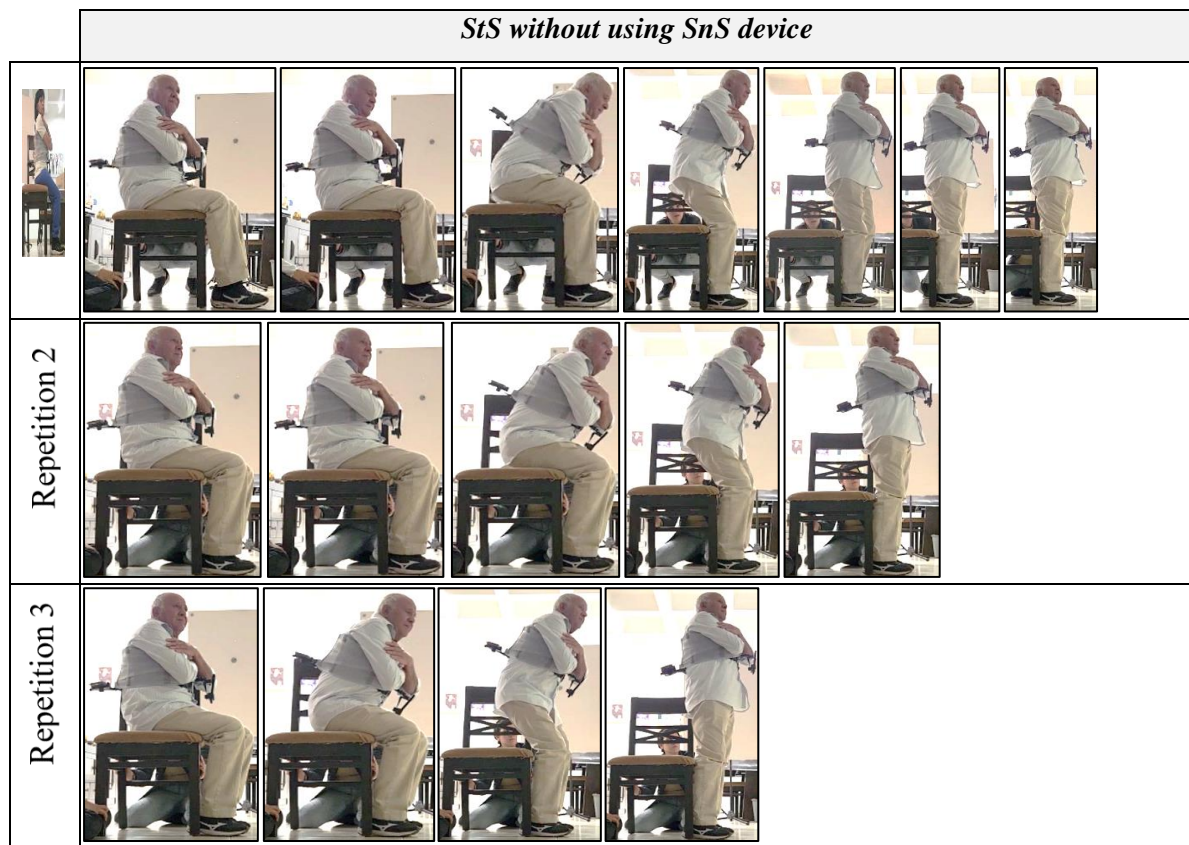


Figure 55 - subject 7 - Selected videos of StS movement without using SnS device

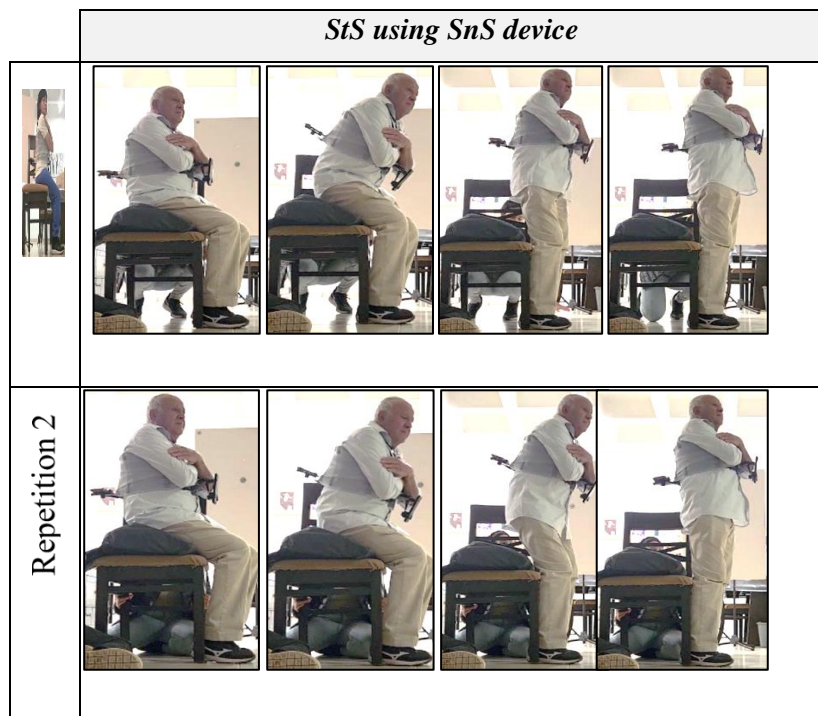




Figure 56 – subject 7 - Selected videos of StS movement using SnS device

From the graphs on Fig.## and Fig.## above, there is an overall resembles in StS movement structure over time in both axes with and without the SnS device. Also, a relation between the axes can be recognized as differences occurred on graph in one axis during the movement at a certain time period, at the same time period a difference can be seen on the other axis. Additionally, the graph of y-axis resembles to the graph on Fig. 2 in the introduction. On y-axis it's very prominent that the starting and ending phases were different for the StS with the SnS compared to those without it. From the pictures it seems that the difference in the end was since without SnS device the back faces backwards. Also, a very good alignment can be recognized between the degree of bending to the height of the peak as in the first repeat without the SnS the bending degree was very dramatic and so the peak. For this subject significant result were seen (Table 4) for AUC in both axes.

9.1.8 Subject 8

x-axis

y-axis

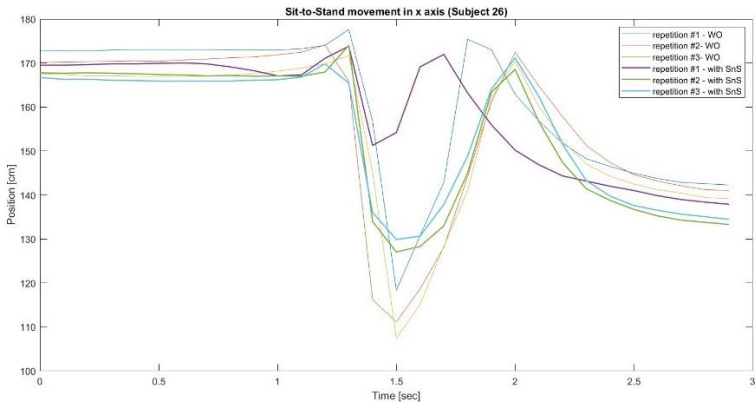


Figure 57 - subject 8 - StS movement of x axis:3 repetitions without using SnS device (blue, red, yellow) ; 3 repetitions using SnS device (bold: purple, green, light blue)

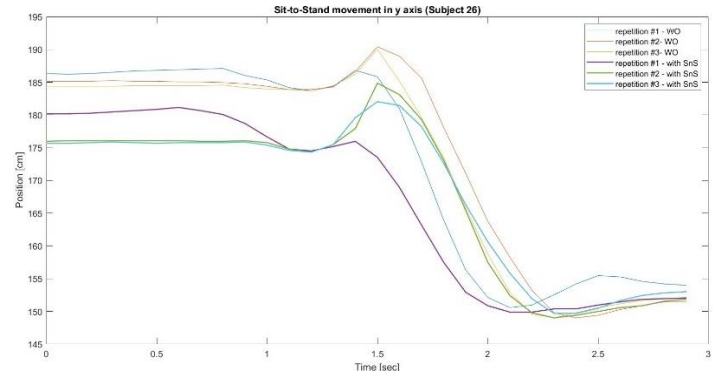


Figure 58 - subject 8 - StS movement of x axis:3 repetitions without using SnS device (blue, red, yellow) ; 3 repetitions using SnS device (bold: purple, green, light blue)

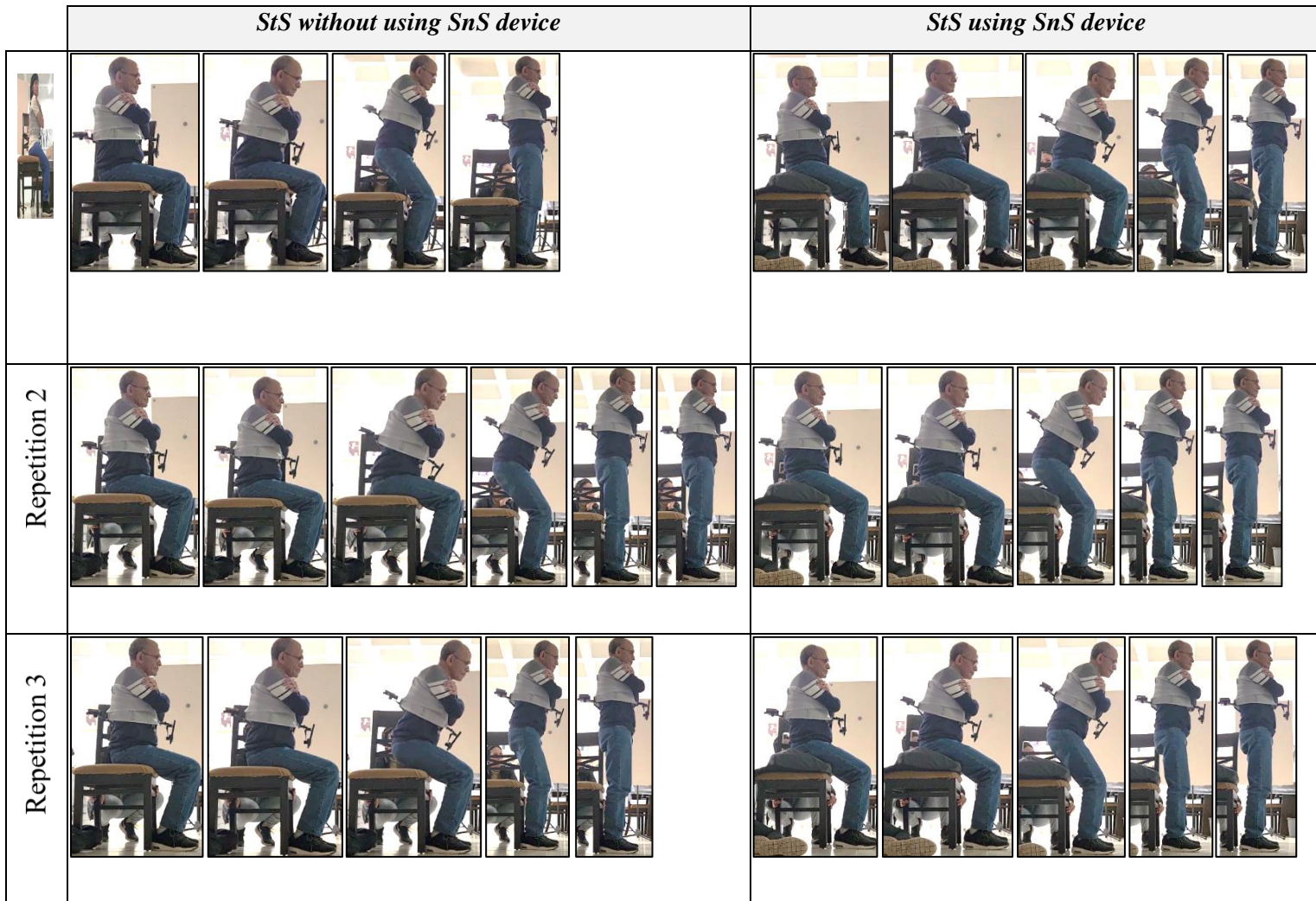


Figure 59 - subject 8 - Selected videos of StS movement with and without using SnS device

From the graphs on Fig.## and Fig.## above, there is an overall resembles in StS movement structure over time in both axes with and without SnS device. Also, a relation between the axes can be recognized as differences occurred on graph in one axis during the movement at a certain time period, at the same time period a difference can be seen on the other axis. Additionally, the graph of y-axis resembles to the graph on Fig. 2 in the introduction. When looking at the attached images on Fig.### it seems as there was a difference between the StS movement within the same state, for example, the degree of torso bending in the first repeat seems much lower than the bending performed on the other repeats in relation to that, in both axes the peaks seem very light compared to the peaks in the other repeats for the first repeat (in purple) on the graphs. It seems that the reason for the difference is in the starting point of the movement. It seems that the preparation phase for the seat off was affected by the starting point, when in the first repetition with SNS device (in purple) there is a more significant peak compared to the starting point because the back was backwards during the sitting. Following this, the least amount of bending appears to be observed for this repeat. Moreover, at the starting point, the distance on the x-axis and y-axis seems to be lower, probably in light of the height of the pillow.

9.2 comprehensive evaluation of the StS movement with the SnS device

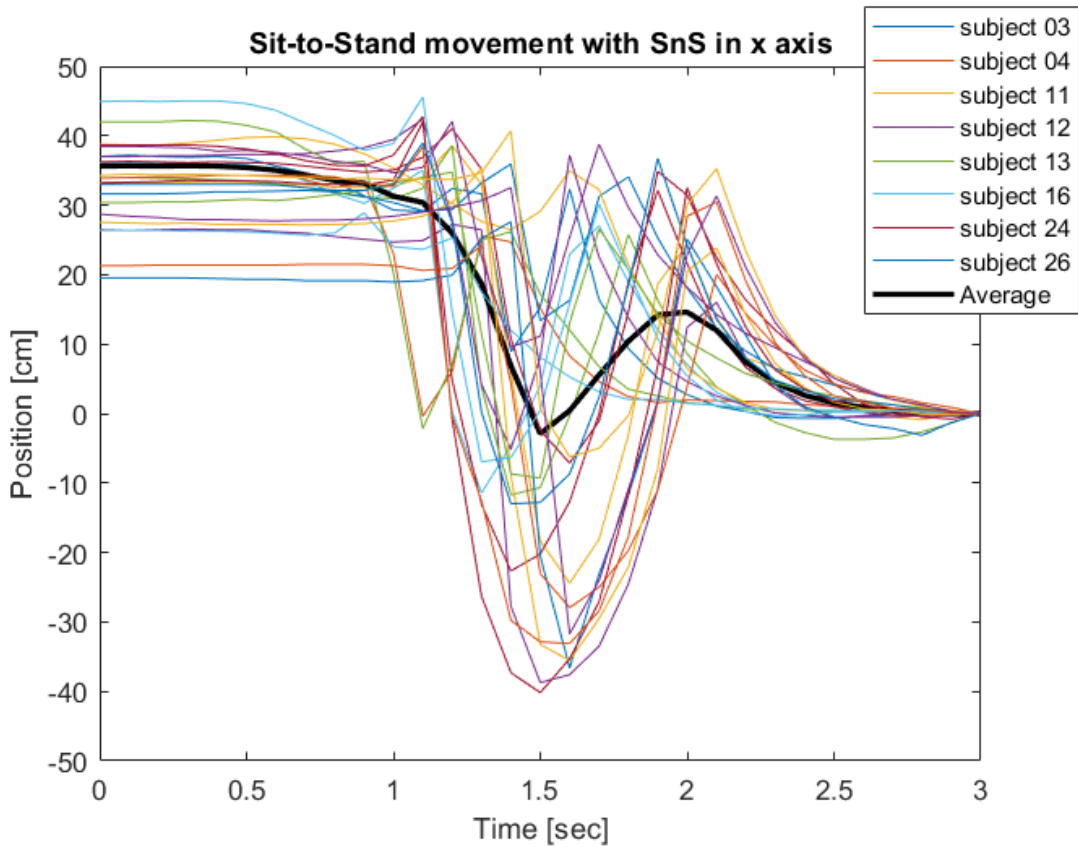


Figure 60 - Model of StS movement of x axis (colorful – all the subjects' measurements, black – the weighted average model)

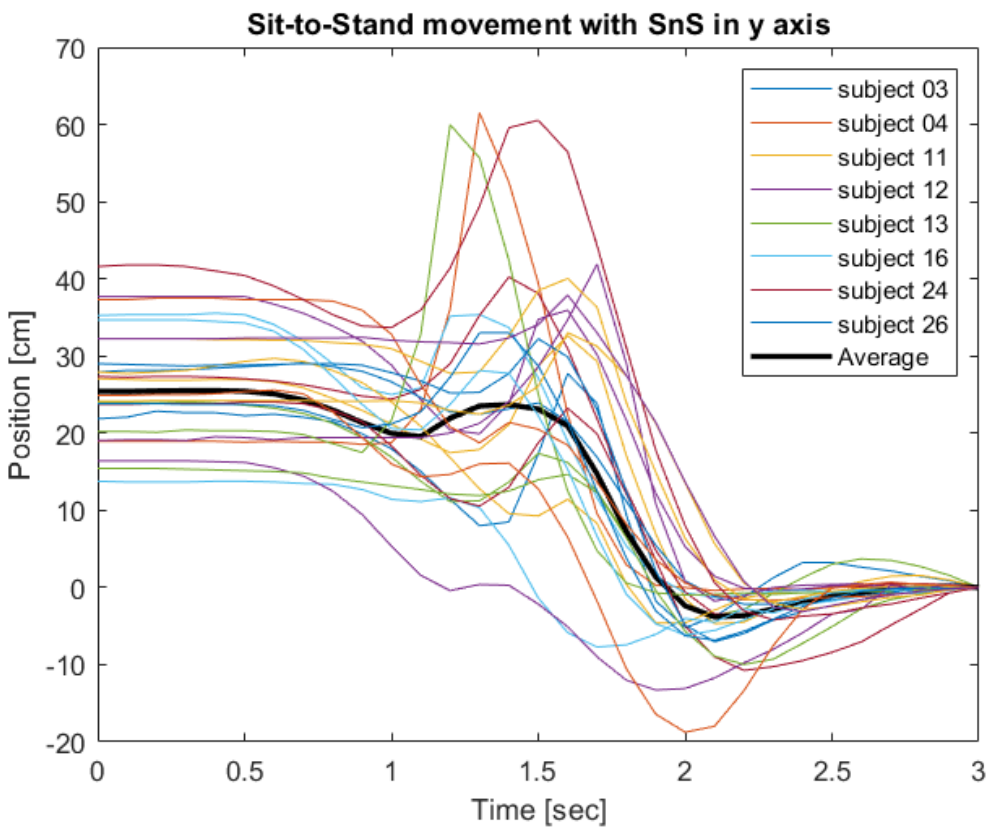


Figure 61 - Model of StS movement of y axis (colorful – all the subjects' measurements, black – the weighted average model)

9.3 MATLAB code for the LiDAR calibration

MATLAB Code	Explanation
<pre>clc ; clear all ; close all ; mainpath = pwd; mainpath = strcat(mainpath,'LiDAR calibration results'); LiDAR_results = dir(fullfile(mainpath, "*LiDAR.csv")); machine_results = dir(fullfile(mainpath, "*machine.csv")); times_mat_Li = { }; positions_mat_Li = { }; velocities_mat_Li = { }; velocity_calc_mat_Li = { }; for file=1:length(LiDAR_results) curr_LiDAR_data = readtable([mainpath, '\',LiDAR_results(file).name]); time_Li = curr_LiDAR_data.time; times_mat_Li{1,file} = time_Li - time_Li(1); position_Li = curr_LiDAR_data.position;</pre>	1. Loading the data from the LiDAR and the Instron machine
	2. Extracting the values obtained by the LiDAR sensor (time, velocity and position)

MATLAB Code	Explanation
<pre> positions_mat_Li{1,file} = position_Li - position_Li(1); velocities_mat_Li{1,file} = curr_LiDAR_data.velocity; velocity_calc_mat_Li{1,file} = position_Li(2:end).*10./time_Li(2:end); end times_mat_ma = {}; positions_mat_ma = {}; velocity_calc_mat_ma = {}; position_errors = {}; velocity_errors = {}; T = []; for file=1:length(machine_results) curr_machine_data = readtable([mainpath,'\',machine_results(file).name]); time_ma = curr_machine_data.Time; times_mat_ma{1,file} = time_ma - time_ma(1); position_ma = curr_machine_data.Displacement; positions_mat_ma{1,file} = position_ma.*0.1 - position_ma(1)*0.1; % from mm to cm velocity_calc_mat_ma{1,file} = position_ma(2:end)./time_ma(2:end); p = polyfit(times_mat_ma{file},positions_mat_ma{file},1); diff_Li = median(diff(positions_mat_Li{1,file})); diff_ma = median(diff(positions_mat_ma{1,file})); sample = diff_Li/diff_ma; positions_mat_ma{1,file} = downsample(positions_mat_ma{1,file},floor(sample*10)); add = abs(size(positions_mat_Li{file},1)-size(positions_mat_ma{file},1)); y = polyval(p,times_mat_Li{file}); positions_Li = positions_mat_Li{file}(2:end); y_new = y(2:end); velocity_calc_Li = velocity_calc_mat_Li{file}(1:end); time_Li = times_mat_Li{file}(2:end); if file == 1 file == 2 x_value = 570; else x_value = 380; end </pre>	<p>3. Extracting the values obtained by the Instron machine (time, velocity and position)</p>

MATLAB Code	Explanation
<pre> idx = find(times_mat_Li{file}>=x_value); time = time_Li(1:idx(1)); position = positions_Li(1:idx(1)); y = y_new(1:idx(1)); % errors calculations: position_errors{1,file} = (abs(position - y).*100)./y; % relative error [%] in position (LiDAR compared to machine) velocity_errors{1,file} = (abs(position./time - y./time)*100)./(y./time); % relative error [%] in velocity (LiDAR com- pared to machine) mean_pos_relative_err = mean(position_errors{file}); STD_pos_err = std(position_errors{file}); mean_vel_relative_err = mean(velocity_errors{file}); STD_vel_err = std(velocity_errors{file}); rmse_pos = sqrt(mean((position - y).^2)); rmse_vel = sqrt(mean((velocity_calc_Li(1:idx(1)) - y./time).^2)); T = [T;table(mean_pos_rel- ative_err,STD_pos_err,rmse_pos,mean_vel_rel- ative_err,STD_vel_err,rmse_vel)]; </pre>	4.Calculating the difference between the results obtained from the LiDAR to those obtained from the Instron and measure the relative error as well as the mean square error.
<pre> figure(file) hold on plot(time,position) plot(time,y) legend('LiDAR','Machine (gold standard)') xlabel('Time [sec]') ylabel('Position [cm]') xlim([0 600]) ylim([0 100]) title(sprintf('Test number %d \nPosition [cm] vs. Time [sec] using Li- DAR and Instron testing machine',file)) hold off end </pre>	5.Plot graphs of the different test set to visualize the outcomes from the two measurements and to able to compare between their trends.

9.4 MATLAB code for the StS analysis

9.4.1 Extract StS sections from the signals

MATLAB Code	Explanation
<pre> function [labelVals,labelLocs,num_sections] = findSTS(raw_sig- nal,time) labelVals = cell(3,1); labelLocs = cell(3,1); % [indeces] </pre>	1.apply low pass filter to smooth the signals and reduce noise

MATLAB Code	Explanation
<pre>window = 5; %% low pass filter filtered_signal = smoothdata(raw_signal,30,"gaussian"); % calculate the first derivative of the signal to extract the locations % where the signal decreases and where it increases diff_sig = movmedian(diff(filtered_signal),window); up_locs = find(diff_sig<0); down_locs = find(diff_sig>0); idx_up=diff(up_locs); gaps_up=unique([find(idx_up>1)' ;numel(up_locs)]); ii1=[1 :gaps_up(1:end-1)+1]; out_up=arrayfun(@(x,y) up_locs(x:y),ii1,gaps_up,'un',0); idx_down=diff(down_locs); gaps_down=unique([find(idx_down>1)' ;numel(down_locs)]); ii2=[1 :gaps_down(1:end-1)+1]; out_down=arrayfun(@(x,y) down_locs(x:y),ii2,gaps_down,'un',0); STS_up_loc = []; STS_up_locs = [];</pre>	2. calculating the first derivative of the signal to extract the locations where the signal decreases and where it increases to be able to extract the StS sections in the signals
	3. Additional filters to better recognize the different section in the signals
<pre>% a matrix that saves the locations where the subject went up (sit to stand). % Each row is a different sit-to-stand movement % The first instant is the begining of the movement and the second instant is where the movement ended. STS_down_loc = []; % same idea only here we ware tracking where the subject went down (stand to sit) [yupper,ylower]=envelope(raw_signal); limit = 17; % mean(yupper) - mean(ylower)- 0.2*mean(mean(yupper),mean(ylower)); for i=1:length(out_up) % take out all elements which their distance in y axis is lower % then the limit and their length is below 0.2 if filtered_signal(out_up{i}(1))-filtered_signal(out_up{i}(end))>=limit && time(out_up{i}(end))-time(out_up{i}(1))>=0.2 STS_up_loc = [STS_up_loc;out_up{i}(1),out_up{i}(end)]; end end for i=1:length(out_down) if filtered_signal(out_down{i}(1))-filtered_signal(out_down{i}(end))>=limit && time(out_down{i}(end))-time(out_down{i}(1))>=0.2 STS_down_loc = [STS_down_loc;out_down{i}(1),out_down{i}(end)]; end end</pre>	

MATLAB Code	Explanation
<pre> STS_up = repmat("STS_up",size(STS_up_loc,1),1); range = 15; for row=1:length(STS_up_loc(:,1)) % take out all elements that the median of the values in the range % before them are not higher then the values in the range after them % and if two adjusent elements are closer then 5 sec to each other % if row~=length(STS_up_loc(:,1)) % if STS_up_loc(row,1)-range>0 && %STS_up_loc(row,2)+range<length(filtered_signal) && %time(STS_up_loc(row+1,1))-time(STS_up_loc(row,2))>5 % if median(filtered_signal(STS_up_loc(row,1)- %range:STS_up_loc(row,1)))>median(filtered_sig- %nal(STS_up_loc(row,2):STS_up_loc(row,2)+range)) STS_up_locs = [STS_up_locs;STS_up_loc(row,1)- range,STS_up_loc(row,2)+range]; end else STS_up_locs = [STS_up_locs;STS_up_loc(row,1),STS_up_loc(row,2)]; end elseif row==length(STS_up_loc(:,1)) && length(STS_up_loc(:,1))>1 if STS_up_loc(row,1)-range>0 && STS_up_loc(row,2)+range<length(filtered_signal) && time(STS_up_loc(row,1))-time(STS_up_loc(row-1,2))>5 if median(filtered_signal(STS_up_loc(row,1)- range:STS_up_loc(row,1)))>median(filtered_sig- nal(STS_up_loc(row,2):STS_up_loc(row,2)+range)) STS_up_locs = [STS_up_locs;STS_up_loc(row,1)- range,STS_up_loc(row,2)+range]; end end else if STS_up_loc(row,1)-range>0 && STS_up_loc(row,2)+range<length(filtered_signal) if median(filtered_signal(STS_up_loc(row,1)- range:STS_up_loc(row,1)))>median(filtered_sig- nal(STS_up_loc(row,2):STS_up_loc(row,2)+range)) STS_up_locs = [STS_up_locs;STS_up_loc(row,1)- range,STS_up_loc(row,2)+range]; end end end end </pre>	<p>4.apply different limitations that were based on the visualization of the data and back and forth session for optimization, this part of the code optimizing the StS definition for the data collected from the experiment.</p>

<i>MATLAB Code</i>	<i>Explanation</i>
<pre> for row=2:length(STS_up_locs(:,1)) if STS_up_locs(row,1)-STS_up_locs(row-1,2)<100 if STS_up_locs(row,2)-STS_up_locs(row-1,1)<200 STS_up_locs(row,:)= [STS_up_locs(row- 1,1),STS_up_locs(row,2)]; STS_up_locs(row-1,:)= [0, 0]; else STS_up_locs(row-1,:)= [0, 0]; end end end STS_up_locs(all(STS_up_locs==0,2),:)= []; STS_up = repmat("STS_up",size(STS_up_locs,1),1); STS_down = repmat("STS_down",size(STS_down_loc,1),1); labelLocs = [STS_up_locs;STS_down_loc]; labelVals = [STS_up;STS_down]; num_sections = size(labelLocs,1); end </pre>	

9.4.2 Calculate the computational assumptions and the statistical measurements

<i>MATLAB Code</i>	<i>Explanation</i>
<pre> function [T_anova] = statistical_calcula- tion(X_wo_1,X_w_1,Y_wo_1,Y_w_1,X_wo_2,X_w_2,Y_wo_2,Y_w_- 2,X_wo_3,X_w_3,Y_wo_3,Y_w_3,subject) %% reordering the data X_wo_1= X_wo_1-X_wo_1(end);X_wo_2= X_wo_2-X_wo_2(end); X_wo_3= X_wo_3-X_wo_3(end); X_w_1= X_w_1-X_w_1(end);X_w_2= X_w_2- X_w_2(end);X_w_3= X_w_3-X_w_3(end); Y_wo_1= Y_wo_1-Y_wo_1(end);Y_wo_2= Y_wo_2- Y_wo_2(end);Y_wo_3= Y_wo_3-Y_wo_3(end); Y_w_1= Y_w_1-Y_w_1(end);Y_w_2= Y_w_2- Y_w_2(end);Y_w_3= Y_w_3-Y_w_3(end); len_X_WO_1 = length(X_wo_1); len_X_WO_2 = length(X_wo_2); len_X_WO_3 = length(X_wo_3); len_X_W_1 = length(X_w_1); len_X_W_2 = length(X_w_2); len_X_W_3 = length(X_w_3); len_Y_WO_1 = length(Y_wo_1); len_Y_WO_2 = length(Y_wo_2); len_Y_WO_3 = length(Y_wo_3); len_Y_W_1 = length(Y_w_1); len_Y_W_2 = length(Y_w_2); len_Y_W_3 = length(Y_w_3); len_vec = [len_X_WO_1,len_X_WO_2,len_X_WO_3,len_X_W_1,len_X_W_2,le </pre>	<p>1.Re-ordering the data</p>

MATLAB Code	Explanation
<pre>n_X_W_3,len_Y_WO_1,len_Y_WO_2,len_Y_WO_3,len_Y_W_1,len_ Y_W_2,len_Y_W_3]; max_len = max(len_vec); NaN_vec = NaN(1,max_len); x_wo_1 = NaN_vec; x_wo_2 = NaN_vec; x_wo_3 = NaN_vec; x_w_1 = NaN_vec; x_w_2 = NaN_vec; x_w_3 = NaN_vec; y_wo_1 = NaN_vec; y_wo_2 = NaN_vec; y_wo_3 = NaN_vec; y_w_1 = NaN_vec; y_w_2 = NaN_vec; y_w_3 = NaN_vec; t = 0:0.1:(max_len-1)*0.1; x_wo_1(1:length(X_wo_1)) = X_wo_1(:); x_wo_2(1:length(X_wo_2)) = X_wo_2(:); x_wo_3(1:length(X_wo_3)) = X_wo_3(:); x_w_1(1:length(X_w_1)) = X_w_1(:); x_w_2(1:length(X_w_2)) = X_w_2(:); x_w_3(1:length(X_w_3)) = X_w_3(:); y_wo_1(1:length(Y_wo_1)) = Y_wo_1(:); y_wo_2(1:length(Y_wo_2)) = Y_wo_2(:); y_wo_3(1:length(Y_wo_3)) = Y_wo_3(:); y_w_1(1:length(Y_w_1)) = Y_w_1(:); y_w_2(1:length(Y_w_2)) = Y_w_2(:); y_w_3(1:length(Y_w_3)) = Y_w_3(:); plot_2d(x_wo_1,x_w_1,y_wo_1,y_w_1,x_wo_2,x_w_2,y_wo_2,y_w_2 ,x_wo_3,x_w_3,y_wo_3,y_w_3,t,subject) groups = {'Without SnS','Without SnS','Without SnS','With SnS','With SnS';</pre>	2. Plotting 2 dimensional graph of the sections with and without SnS
<pre>t = time(seg.beg:seg.end); x_wo_1 = x_wo(seg.beg:seg.end); x_wo_2 = x_wo(seg.beg:seg.end); x_wo_3 = x_wo(seg.beg:seg.end); x_w_1 = x_w(seg.beg:seg.end); x_w_2 = x_w(seg.beg:seg.end); x_w_3 = x_w(seg.beg:seg.end); y_wo_1 = y_wo(seg.beg:seg.end); y_wo_2 = y_wo(seg.beg:seg.end); y_wo_3 = y_wo(seg.beg:seg.end); y_w_1 = y_w(seg.beg:seg.end); y_w_2 = y_w(seg.beg:seg.end); y_w_3 = y_w(seg.beg:seg.end); figure(5); plot(t,x_wo_1); hold on ; plot(t,x_wo_2); hold on ; plot(t,x_wo_3); hold on ; plot(t,x_w_1,'LineWidth',1.2); hold on ; plot(t,x_w_2,'LineWidth',1.2); hold on ; plot(t,x_w_3,'LineWidth',1.2); hold on ; title('Sit-to-Stand movement in x axis (examinee 03)') xlabel('Time [sec]') ylabel('Position [cm]')</pre>	3.Extracting the relevant segments (transition from sitting to standing) Based on the graphs from step 2.
	Suppose there are 3 repetitions of an experiment. 4 types of segments are extracte from each repetition: - x_wo = Movement (position) on x axis without using SnS device. - x_w = Movement (position) on x axis using SnS device. - y_wo = Movement (position) on y axis without using SnS device. - y_w = Movement (position) on y axis using SnS device. For each segment a times vector will be adjusted. A particular time vector may fit into more than one segment (depending on the length of the segments).
	4.Optimizing the extracted segments & plotting The segments extracted in stage 3 will be optimized, by drawing the segments (of the same axis) on the same figure and moving them on the axis accordingly. At the end of the Optimizing process, the final graphs will be drawn with the appropriate titles and legend.

MATLAB Code	Explanation
<pre>legend('repetition #1 - WO','repetition #2- WO','repetition #3- WO','re- petition #1 - with SnS','repetition #2 - with SnS','repetition #3 - with SnS') figure(6); plot(t2,y_wo_1); hold on ; plot(t2,y_wo_2); hold on ; plot(t2,y_wo_3); hold on plot(t2,y_w_1,'LineWidth',1.2); hold on ; plot(t2,y_w_2,'Lin- eWidth',1.2); hold on ; plot(t2,y_w_3,'LineWidth',1.2); hold on; title('Sit-to-Stand movement in y axis (examinee 03)') xlabel('Time [sec]') ylabel('Position [cm]') legend('repetition #1 - WO','repetition #2- WO','repetition #3- WO','re- petition #1 - with SnS','repetition #2 - with SnS','repetition #3 - with SnS')</pre>	
<pre>auc_x_wo_1=trapz(x_wo_1); auc_x_wo_2=trapz(x_wo_2); auc_x_wo_3=trapz(x_wo_3); auc_x_w_1=trapz(x_w_1); auc_x_w_2=trapz(x_w_2); auc_x_w_3=trapz(x_w_3); [h_AUC_x,p_AUC_x] = ttest2([auc_x_wo_1,auc_x_wo_2,auc_x_wo_3],[auc_x_w_1,auc_x_w_- 2,auc_x_w_3],'Alpha',0.05); auc_x_wo_avg = mean([auc_x_wo_1,auc_x_wo_2,auc_x_wo_3]); auc_x_w_avg = mean([auc_x_w_1,auc_x_w_2,auc_x_w_3]); diff_auc_x = ((auc_x_w_avg-auc_x_wo_avg)/auc_x_wo_avg)*100; disp('AUC x') ; sprintf('%f \n%f',p_AUC_x,diff_auc_x) auc_y_wo_1=trapz(y_wo_1); auc_y_wo_2=trapz(y_wo_2); auc_y_wo_3=trapz(y_wo_3); auc_y_w_1=trapz(y_w_1); auc_y_w_2=trapz(y_w_2); auc_y_w_3=trapz(y_w_3); [h_AUC_y,p_AUC_y] = ttest2([auc_y_wo_1,auc_y_wo_2,auc_y_wo_3],[auc_y_w_1,auc_y_w_- 2,auc_y_w_3],'Alpha',0.05); auc_y_wo_avg = mean([auc_y_wo_1,auc_y_wo_2,auc_y_wo_3]); auc_y_w_avg = mean([auc_y_w_1,auc_y_w_2,auc_y_w_3]); diff_auc_y = ((auc_y_w_avg-auc_y_wo_avg)/auc_y_wo_avg)*100; disp('AUC y') ; sprintf('%f \n%f',p_AUC_y,diff_auc_y)</pre>	<p>5.Calculation of computational assumptions</p> <p>5.1.AUC</p> <p>For each segment AUC was calculated (by the function trapz). Between the segments of the same axis, the significance of the results was calculated by the t-test. Also, the average was calculated for each type of segment (of the 4 types mentioned above). A relative error was calculated between the averages.</p>
<pre>%Position_x set1_data_position_x_wo = [x_wo_1',x_wo_2',x_wo_3']; set2_data_position_x_w = [x_w_1',x_w_2',x_w_3']; p_value_position_anova_x = anova1([set1_data_position_x_wo, set2_data_position_x_w], groups,'off'); %Position_y set1_data_position_y_wo = [y_wo_1',y_wo_2',y_wo_3']; set2_data_position_y_w = [y_w_1',y_w_2',y_w_3']; p_value_position_anova_y = anova1([set1_data_position_y_wo, set2_data_position_y_w], groups,'off');</pre>	<p>6. Position</p> <p>For each segment the velocity was calculated (by subtracting between consecutive positions. The average is calculated for each vector (in its absolute values). Between the segments of the same axis, the significance of the results was calculated by the ANOVA test. Also, the average was calculated for each type of segment (of the 4 types mentioned above - in this case on the averages of the original vectors). A relative error was calculated between the averages.</p>
<pre>%VELOCITY_X</pre>	<p>7. VELOCITY</p>

MATLAB Code	Explanation
<pre> vel_x_wo_1 = diff(X_wo_1)./0.1 ; vel_x_wo_2 = diff(X_wo_2)./0.1 ; vel_x_wo_3 = diff(X_wo_3)./0.1; vel_x_w_1 = diff(X_w_1)./0.1 ; vel_x_w_2 = diff(X_w_2)./0.1 ; vel_x_w_3 = diff(X_w_3)./0.1; set1_data_vel_x_wo = [vel_x_wo_1,vel_x_wo_2,vel_x_wo_3]; set2_data_vel_x_w = [vel_x_w_1,vel_x_w_2,vel_x_w_3]; p_value_vel_anova_x = anova1([set1_data_vel_x_wo, set2_data_vel_x_w], groups,'off'); % VELOCITY_ vel_y_wo_1 = diff(Y_wo_1)./0.1 ; vel_y_wo_2 = diff(Y_wo_2)./0.1 ; vel_y_wo_3 = diff(Y_wo_3)./0.1; vel_y_w_1 = diff(Y_w_1)./0.1 ; vel_y_w_2 = diff(Y_w_2)./0.1 ; vel_y_w_3 = diff(Y_w_3)./0.1; set1_data_vel_y_wo = [vel_y_wo_1,vel_y_wo_2,vel_y_wo_3]; set2_data_vel_y_w = [vel_y_w_1,vel_y_w_2,vel_y_w_3]; p_value_vel_anova_y = anova1([set1_data_vel_y_wo, set2_data_vel_y_w], groups,'off'); </pre>	<p>For each segment the velocity was calculated (by subtracting between consecutive positions and dividing by the time interval (0.1 seconds)). Then, for each velocity vector obtained, an absolute value was calculated. The average is calculated for each vector (in its absolute values). Between the segments of the same axis, the significance of the results was calculated by the ANOVA test. Also, the average was calculated for each type of segment (of the 4 types mentioned above - in this case on the averages of the original vectors). A relative error was calculated between the averages.</p>

<pre> % ACCELERATION_X accel_x_wo_1 = diff(diff(X_wo_1)./0.1)./0.1 ; accel_x_wo_2 = diff(diff(X_wo_2)./0.1)./0.1 ; accel_x_wo_3 = diff(diff(X_wo_3)./0.1)./0.1; accel_x_w_1 = diff(diff(X_w_1)./0.1)./0.1 ; accel_x_w_2 = diff(diff(X_w_2)./0.1)./0.1 ; accel_x_w_3 = diff(diff(X_w_3)./0.1)./0.1; set1_data_accel_x_wo = [accel_x_wo_1,accel_x_wo_2,ac- cel_x_wo_3]; set2_data_accel_x_w = [accel_x_w_1,accel_x_w_2,accel_x_w_3]; p_value_accel_anova_x = anova1([set1_data_accel_x_wo, set2_data_accel_x_w], groups,'off'); % ACCELERATION_y accel_y_wo_1 = diff(diff(Y_wo_1)./0.1)./0.1 ; accel_y_wo_2 = diff(diff(Y_wo_2)./0.1)./0.1 ; accel_y_wo_3 = diff(diff(Y_wo_3)./0.1)./0.1; accel_y_w_1 = diff(diff(Y_w_1)./0.1)./0.1 ; accel_y_w_2 = diff(diff(Y_w_2)./0.1)./0.1 ; accel_y_w_3 = diff(diff(Y_w_3)./0.1)./0.1; set1_data_accel_y_wo = [accel_y_wo_1,accel_y_wo_2,ac- cel_y_wo_3]; set2_data_accel_y_w = [accel_y_w_1,accel_y_w_2,accel_y_w_3]; p_value_accel_anova_y = anova1([set1_data_accel_y_wo, set2_data_accel_y_w], groups,'off'); %% results T_anova = table(p_value_position_anova_x,p_value_posi- tion_anova_y, p_value_vel_anova_x,p_value_vel_anova_y,p_value_ac- cel_anova_x,p_value_accel_anova_y); filename = 'SnS_Results_vell_accel_anova.xlsx'; writetable(T_anova,filename,'Sheet',1); </pre>	<p>8. ACCELERATION</p> <p>For each segment the acceleration was calculated (by subtracting between consecutive velocity and dividing by the time interval (0.1 seconds)). Then, for each acceleration vector obtained, an absolute value was calculated. The average is calculated for each vector (in its absolute values). Between the segments of the same axis, the significance of the results was calculated by the ANOVA test. Also, the average was calculated for each type of segment (of the 4 types mentioned above - in this case on the averages of the original vectors). A relative error was calculated between the averages.</p> <p>9. The results of the ANOVA test were saved in a table</p>
--	--

MATLAB Code	Explanation
end	

9.4.3 Plot 2 dimensional graphs

MATLAB Code	Explanation
function	
plot_2d(x_wo_1,x_w_1,y_wo_1,y_w_1,x_wo_2,x_w_2,y_wo_2,y_w_2 ,x_wo_3,x_w_3,y_wo_3,y_w_3,t,subject)	
figure;	1. Plotting the repetitions in x axis with and without SnS
p1 = plot(t,x_wo_1); p1.Color = '#0072BD'; p1.LineStyle = '-'; hold on ;	
p2 = plot(t,x_wo_2); p2.Color = '#0072BD'; p2.LineStyle = '-'; hold on ;	
p3 = plot(t,x_wo_3); p3.Color = '#0072BD'; p3.LineStyle = '-'; hold on ;	
p1 = plot(t,x_w_1); p1.Color = '#D95319'; p1.LineStyle = '-'; hold on ;	
p2 = plot(t,x_w_2); p2.Color = '#D95319'; p2.LineStyle = '-'; hold on ;	
p3 = plot(t,x_w_3); p3.Color = '#D95319'; p3.LineStyle = '-'; hold on ;	
title(['Sit-to-Stand movement in x axis (Subject ',subject,')'])	
xlabel('Time [sec]')	
ylabel('Position [cm]')	
hline = reffline(0, 0);	
hline.Color = 'k';	
legend('Repetition 1 - Without SnS','Repetition 2 - Without SnS','Repetition 3 - Without SnS','Repetition 1 - with SnS','Repetition 2 - with SnS','Repetition 3 - with SnS')	
figure;	2. Plotting the repetitions in y axis with and without SnS
p1 = plot(t,y_wo_1); p1.Color = '#0072BD'; p1.LineStyle = '-'; hold on ;	
p2 = plot(t,y_wo_2); p2.Color = '#0072BD'; p2.LineStyle = '-'; hold on ;	
p3 = plot(t,y_wo_3); p3.Color = '#0072BD'; p3.LineStyle = '-'; hold on ;	
p1 = plot(t,y_w_1); p1.Color = '#D95319'; p1.LineStyle = '-'; hold on ;	
p2 = plot(t,y_w_2); p2.Color = '#D95319'; p2.LineStyle = '-'; hold on ;	
p3 = plot(t,y_w_3); p3.Color = '#D95319'; p3.LineStyle = '-'; hold on ;	

<i>MATLAB Code</i>	<i>Explanation</i>
<pre> title(['Sit-to-Stand movement in y axis (Subject ',subject,')']) xlabel('Time [sec]') ylabel('Position [cm]') hline = refline(0, 0); hline.Color = 'k'; legend('Repetition 1 - Without SnS','Repetition 2- Without SnS','Re- petition 3- Without SnS','Repetition 1 - with SnS','Repetition 2 - with SnS','Repetition 3 - with SnS') end </pre>	